

(Arylimido)niobium(V) Complexes Containing 2-Pyridylmethylanylido Ligand as Catalyst Precursors for Ethylene Dimerization That Proceeds via Cationic Nb(V) Species

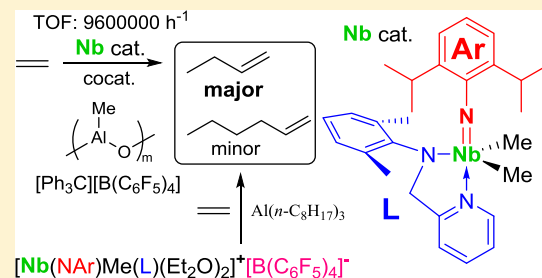
Masaharu Kuboki and Kotohiro Nomura*[✉]

Department of Chemistry, Graduate School of Science, Tokyo Metropolitan University, 1-1 Minami Osawa, Hachioji, Tokyo 192-0397, Japan

Supporting Information

ABSTRACT: (Arylimido)niobium(V) complexes containing 2-pyridylmethylanylido ligand Nb(NAr)X₂(L) [L = 2-(2,6-Me₂C₆H₃)-NCH₂(C₅H₄N); X = NMe₂ (2a,b), OCH(CF₃)₂ (3a–c), Me (4a–c), CH₂SiMe₃ (5a); Ar = 2,6-Me₂C₆H₃ (a), 2,6-ⁱPr₂C₆H₃ (b), 2-MeC₆H₄ (c)] have been prepared, and structures of 3a,b, 4b, and 5a were determined by X-ray crystallography. The dimethyl complexes (4a,b) exhibited catalytic activities for ethylene dimerization in the presence of methylaluminoxane (MAO), whereas the activity by 4c was negligible under the same conditions. Complex 4b showed the highest activity, and the activity at 50 °C was higher than those conducted at 25 and 80 °C.

The major product was 1-butene, and 1-hexene was formed by subsequent reaction of ethylene with 1-butene accumulated in the reaction mixture. A first-order relationship between the activity [turnover frequency (TOF)] and ethylene pressure was observed, suggesting that the metal-alkyl species would play a role in this catalysis. The activities further increased remarkably upon addition of [Ph₃C][B(C₆F₅)₄] at 50 °C; TOF at the initial stage (5 min) of 2 100 000 h⁻¹ (583 s⁻¹) has been attained. Reactions of the dimethyl complexes (4a,b) with 1.0 equiv of [Ph₃C][B(C₆F₅)₄] in Et₂O afforded [Nb(NAr)Me(L)]⁺[B(C₆F₅)₄]⁻(Et₂O)₂ (6a,b), and the reaction of 6b with ethylene afforded 1-butene and 1-hexene even in the absence of MAO, clearly suggesting that the cationic species play a role in this catalysis. X-ray absorption near edge structure spectra of the catalyst solutions containing 4b (in toluene at 25 °C) and MAO (10 and 50 equiv) showed no significant differences in the pre-edge peak positions and intensities from that in the dimethyl complex (4b), strongly suggesting that both the oxidation states and the basic structures are maintained upon addition of MAO in these catalyst solutions.



1. INTRODUCTION

Ethylene oligomerization for production of linear α -olefins, exemplified by nickel complex catalysts containing a chelate P–O ligand (in shell higher olefin process, SHOP),¹ is the key reaction in chemical industry^{1,2} and the subject on design of the efficient (highly active and selective) catalysts thus attracts considerable attention in the field of catalysis and organometallic chemistry.^{1–8} Many reports using nickel,^{1,2c,h,3b–d} iron and cobalt,^{2g,i–k,3e,f} chromium,^{2d–f,3a} or titanium complex catalysts⁴ have been known, but the reports using group 5 complex catalysts,^{5–8} in particular, homogeneous niobium complex catalysts, have been limited (especially in recent 30 years).⁷

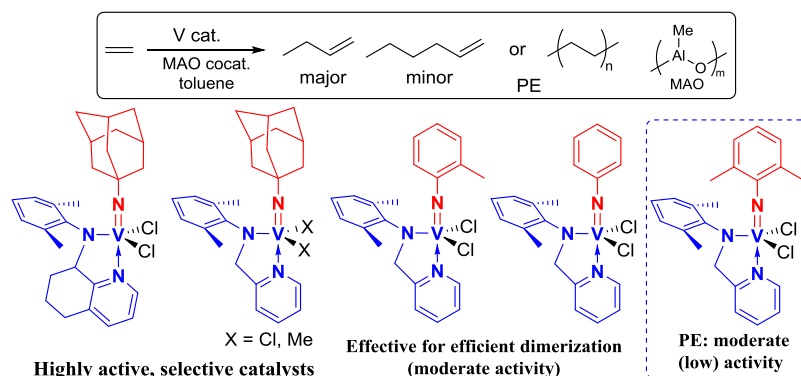
(Imido)Vanadium(V) complexes containing 2-pyridylmethylanylido or 5,6,7-trihydroquinolyl-8-anilido ligands, V(NR′)-Cl₂[2-(2,6-Me₂C₆H₃)NCH₂(C₅H₄N)] or V(NR′)Cl₂[8-(2,6-Me₂C₆H₃)N(C₉H₁₀N)] [R′ = 1-adamantyl (Ad), 2-MeC₆H₄, C₆H₅, etc.], have been known to exhibit remarkably high both activities and selectivity for ethylene dimerization in the presence of the methylaluminoxane (MAO) cocatalyst (Scheme 1).⁶ It was demonstrated that a steric bulk in the imido ligand affects the ethylene reactivity (dimerization or polymerization).^{6a} On the basis of some reaction chemistry (isolation

of cationic methyl complex, confirmation of the catalyst performance with the dimethyl complex, ethylene pressure dependence and effect of Al cocatalyst),⁵¹V NMR and ESR spectra of the catalyst solution, and the solution phase V K edge XAS [X-ray absorption spectroscopy; XANES (X-ray Absorption Near Edge Structure) and FT-extended X-ray absorption fine structure] analysis, it was concluded that the cationic vanadium(V) species play a role in this catalysis.^{6e}

The arylimido ligand has been used to stabilize the high oxidation state early transition-metal complexes, which are often used as the catalysts or catalyst precursors in olefin metathesis and olefin insertion polymerization.⁹ Synthesis and some reaction chemistry of (arylimido)niobium complexes have thus also been known,^{10,11} however, there are no examples applied to catalyst precursors for ethylene oligomerization, whereas (arylimido)niobium(V)–alkylidene complexes exhibit unique characteristics as catalysts for olefin metathesis polymerization.¹¹ Because of promising characteristics demonstrated in the above-mentioned (imido)vanadium(V) complexes containing 2-pyridylmethylanylido ligand (shown in Scheme 1),⁶ we

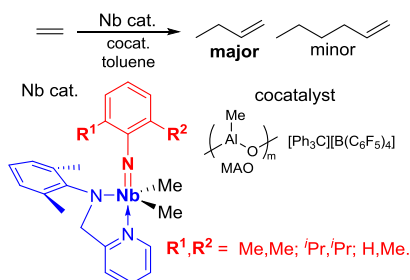
Received: January 14, 2019

Scheme 1. Ethylene Dimerization (Polymerization) Using (Imido)Vanadium(V) Complex Catalysts in the Presence of MAO Cocatalyst⁶



thus have an interest for synthesis of the niobium analogues, especially the dimethyl complexes (Scheme 2), as catalysts for reaction with ethylene.

Scheme 2. Ethylene Oligomerization Using Nb(NAr)Me₂[2-(2,6-Me₂C₆H₃)NCH₂(C₅H₄N)] (Ar = 2,6-Me₂C₆H₃, 2,6-ⁱPr₂C₆H₃, 2-MeC₆H₄) in the Presence of Cocatalysts



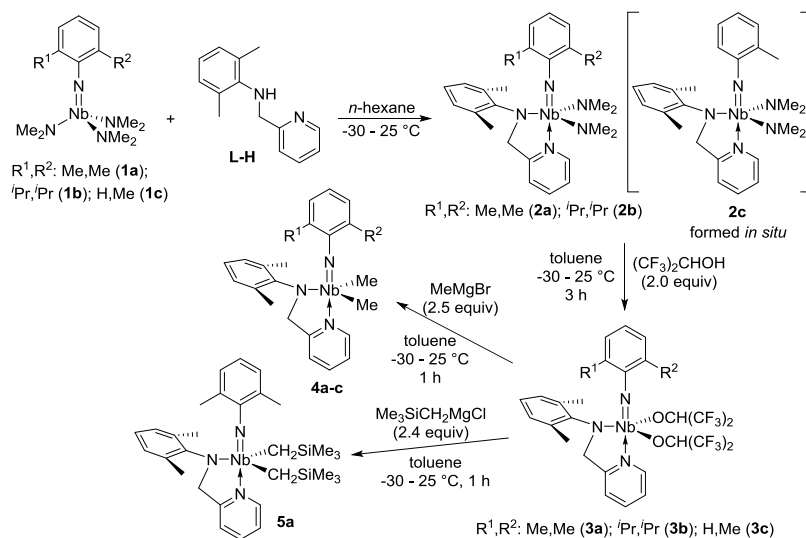
We herein present synthesis and structural analysis of (arylimido)niobium(V) complexes containing 2-pyridylmethyl-anilido ligands, Nb(NAr)X₂[2-(2,6-Me₂C₆H₃)-NCH₂(C₅H₄N)] [Ar = 2,6-Me₂C₆H₃, 2,6-ⁱPr₂C₆H₃, 2-MeC₆H₄]

MeC₆H₄; X = NMe₂, OCH(CF₃)₂, Me, CH₂SiMe₃] (Scheme 2). We wish to demonstrate that Nb(N-2,6-ⁱPr₂C₆H₃)Me₂[2-(2,6-Me₂C₆H₃)NCH₂(C₅H₄N)] exhibits notable catalytic activity for ethylene dimerization in the presence of MAO especially at 50 °C and both the activity and selectivity of oligomer further increased with addition of [Ph₃C][B(C₆F₅)₄]. On the basis of isolation of cationic complexes and the reaction with ethylene, as well as XANES analysis of the catalyst solution, we herein propose the catalytically active species in this catalysis.¹²

2. RESULTS AND DISCUSSION

2.1. Synthesis and Structural Analysis of Nb(NAr)X₂[2-(2,6-Me₂C₆H₃)NCH₂(C₅H₄N)] [Ar = 2,6-Me₂C₆H₃, 2,6-ⁱPr₂C₆H₃, 2-MeC₆H₄; X = NMe₂, OCH(CF₃)₂, Me, CH₂SiMe₃]. The (arylimido)niobium(V)tris(dimethylamide) complexes, Nb(NAr)(NMe₂)₃ [Ar = 2,6-Me₂C₆H₃ (1a), 2,6-ⁱPr₂C₆H₃ (1b), 2-MeC₆H₄ (1c), Scheme 3], have been chosen as the starting complexes for the syntheses of the dimethyl complexes, Nb(NAr)Me₂[2-(2,6-Me₂C₆H₃)-NCH₂(C₅H₄N)] (4a–c, shown in Schemes 2 and 3) because 1b is known as a solvent-free four coordinate (arylimido)-niobium(V) complex,^{11c} which folds a distorted tetrahedral

Scheme 3. Synthesis of Nb(NAr)Me₂[2-(2,6-Me₂C₆H₃)NCH₂(C₅H₄N)] [Ar = 2,6-Me₂C₆H₃ (4a), 2,6-ⁱPr₂C₆H₃ (4b), 2-MeC₆H₄ (4c)] and Nb(N-2,6-Me₂C₆H₃)(CH₂SiMe₃)₂[2-(2,6-Me₂C₆H₃)NCH₂(C₅H₄N)] (5a); Detailed Synthetic Procedures are Described in the Experimental Section, and Selected NMR Spectra are Shown in the Supporting Information¹⁴



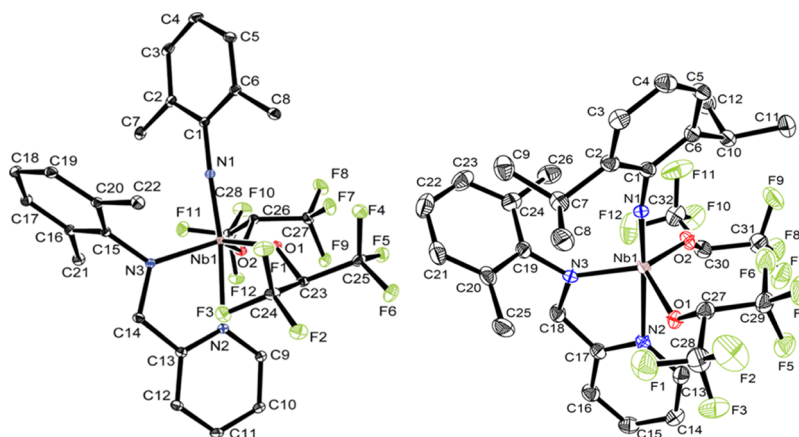


Figure 1. ORTEP drawings for Nb(N-2,6-Me₂C₆H₃)[OCH(CF₃)₂]₂[2-(2,6-Me₂C₆H₃)NCH₂(C₅H₄N)] (**3a**, left) and Nb(N-2,6-ⁱPr₂C₆H₃)[OCH(CF₃)₂]₂[2-(2,6-Me₂C₆H₃)NCH₂(C₅H₄N)] (**3b**, right). Thermal ellipsoids are drawn at 30% probability level, and H atoms were omitted for clarity.¹⁶ Selected bond distances (Å) in **3a**: Nb–O(1) 1.9743(17), Nb–O(2) 1.9769(17), Nb–N(1) 1.7913(19), Nb–N(2) 2.3415(19), Nb–N(3) 1.991(2), N(1)–C(1) 1.388(3). Selected bond angles (°) in **3a**: Nb–N(1)–C(1) 177.24(17), N(1)–Nb–N(2) 172.21(8), N(1)–Nb–N(3) 99.35(9), N(2)–Nb–N(3) 74.92(8), O(1)–Nb–O(2) 116.92(7), O(1)–Nb–N(3) 115.58(8), O(2)–Nb–N(3) 118.60(8), Nb–O(1)–C(23) 142.56(15), Nb–O(2)–C(26) 131.24(15). $\tau = (\beta - \alpha)/60 = (172.21 - 118.60)/60 = 0.894$.¹⁷ Selected bond distances (Å) in **3b**: Nb–O(1) 1.9875(17), Nb–O(2) 1.9618(15), Nb–N(1) 1.7899(17), Nb–N(2) 2.3475(17), Nb–N(3) 1.9891(19), N(1)–C(1) 1.402(3). Selected bond angles (°) in **3b**: Nb–N(1)–C(1) 169.53(17), N(1)–Nb–N(2) 173.37(8), N(1)–Nb–N(3) 103.12(8), N(2)–Nb–N(3) 75.38(7), O(1)–Nb–O(2) 117.93(7), O(1)–Nb–N(3) 117.50(7), O(2)–Nb–N(3) 114.66(7), Nb–O(1)–C(27) 127.96(14), Nb–O(2)–C(30) 143.75(14). $\tau = (\beta - \alpha)/60 = (173.37 - 117.93)/60 = 0.924$.¹⁷

geometry around Nb. This is also because, as reported previously,^{11j} it seemed difficult to remove coordinated solvent (such as 1,2-dimethoxyethane, dme) from the trichloride analogues, Nb(NAr)Cl₃(dme).^{11j,13} Complexes **1a** and **1c** could be prepared according to the analogous procedure for **1b**^{11c} and were used for the next step without further purifications (as described in the [Experimental Section](#)).

It turned out that reactions of Nb(NAr)(NMe₂)₃ (**1a,b**) with 2-(2,6-Me₂C₆H₃)N(H)CH₂(C₅H₄N) (LH) in *n*-hexane afforded corresponding bis(amide) complexes, Nb(NAr)(NMe₂)₂(L) [**2a,b**; L = 2-(2,6-Me₂C₆H₃)NCH₂(C₅H₄N)], by amine (HNMe₂) elimination.¹⁴ The *o*-tolylimido analogue (**2c**) could also be obtained from **1c** by treating with L–H (confirmed formation by ¹H NMR spectrum and was used for the next step without further purification, as described in the [Experimental Section](#)). Attempt for the synthesis of the dichloride complexes from **2b** by treating with excess Me₃SiCl (5 equiv, –30 to 25 °C, overnight)¹⁵ recovered **2b**. In contrast, treatments of **2a,b** with 2.0 equiv of (CF₃)₂CHOH gave the corresponding bis(alkoxide) complexes, Nb(NAr)[OCH(CF₃)₂]₂(L) (**3a,b**) in high yields (85.2, 77.8%, respectively).¹⁴ Analytically pure Nb(N-2-MeC₆H₄)[OCH(CF₃)₂]₂(L) (**3c**) could also be isolated by treating **2c** with 2.0 equiv of (CF₃)₂CHOH. Complexes **3a,b** and **3c** were isolated as white-yellow microcrystals, and structures of **3a,b** were determined by X-ray crystallographic analysis (shown below as [Figure 1](#)).¹⁶ Complexes **2a,b** and **3a–c** were identified by NMR spectra and elemental analysis.¹⁴

Reactions of **3a,b** and **3c** with MeMgBr (2.5 equiv) in toluene yielded the corresponding dimethyl complexes, Nb(NAr)Me₂(L) (**4a–c**). Complexes **4a,b** and **4c** were identified by NMR spectra and elemental analysis,¹⁴ and the structure of **4b** could be determined by X-ray crystallography (shown below, [Figure 2](#)).¹⁶ The structure of **4c** could also be confirmed by X-ray crystallographic analysis.¹⁶ Similarly, treatment of **4a** with Me₃SiCH₂MgCl (2.4 equiv) afforded another dialkyl complex, Nb(N-2,6-Me₂C₆H₃)(CH₂SiMe₃)₂(L) (**5a**). Complex **5a** could

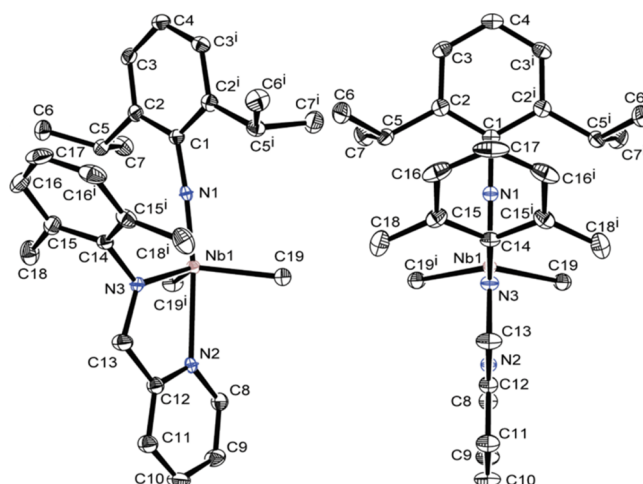


Figure 2. ORTEP drawings for Nb(N-2,6-ⁱPr₂C₆H₃)Me₂[2-(2,6-Me₂C₆H₃)NCH₂(C₅H₄N)] (**4b**). Thermal ellipsoids are drawn at 30% probability level, and H atoms were omitted for clarity.¹⁶ Selected bond distances (Å): Nb–C(19) 2.195(2), Nb–N(1) 1.800(2), Nb–N(2) 2.385(2), Nb–N(3) 2.012(3). Selected bond angles (°): Nb–N(1)–C(1) 174.2(2), N(1)–Nb–N(2) 169.74(10), N(1)–Nb–N(3) 96.73(10), N(2)–Nb–N(3) 73.00(9), C(19)–Nb–C(19ⁱ) 111.71(9), C(19)–Nb–N(1) 101.38(7), C(19)–Nb–N(2) 84.23(7), C(19)–Nb–N(3) 119.91(7). $\tau = (\beta - \alpha)/60 = (169.74 - 111.71)/60 = 0.967$.

be identified by NMR spectra and elemental analysis,¹⁴ and the structure could be determined by the X-ray crystallographic analysis (shown below, [Figure 3](#)).¹⁶ Attempt for the synthesis of (arylimido)niobium(V)–alkylidene complex from **5a** in the presence of 12 equiv of PMe₃ (by α -hydrogen abstraction, at 25 °C for 22 h and 80 °C for 37 h) recovered **5a**.¹⁴

[Figure 1](#) shows Oak Ridge thermal ellipsoid plot (ORTEP) drawings of Nb(NAr)[OCH(CF₃)₂]₂(L) (**3a,b**).¹⁶ These complexes fold a distorted trigonal bipyramidal geometry around niobium with the pyridyl N donor of the bidentate 2-

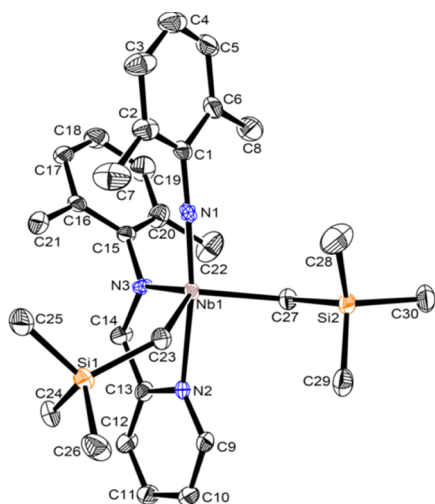


Figure 3. ORTEP drawings for $\text{Nb}(\text{N}-2,6\text{-Me}_2\text{C}_6\text{H}_3)(\text{CH}_2\text{SiMe}_3)_2[2\text{-}(2,6\text{-Me}_2\text{C}_6\text{H}_3)\text{NCH}_2(\text{C}_5\text{H}_4\text{N})]$ (**5a**). Thermal ellipsoids are drawn at 30% probability level, and H atoms were omitted for clarity.¹⁶ Selected bond distances (Å): Nb–C(23) 2.179(3), Nb–C(27) 2.196(3), Nb–N(1) 1.796(2), Nb–N(2) 2.407(2), Nb–N(3) 2.0195(19). Selected bond angles (°): Nb–N(1)–C(1) 177.38(16), N(1)–Nb–N(2) 170.80(7), N(1)–Nb–N(3) 98.59(9), N(2)–Nb–N(3) 72.73(7), C(23)–Nb–C(27) 114.15(9), C(23)–Nb–N(1) 101.57(10), C(23)–Nb–N(2) 81.33(8), C(23)–Nb–N(3) 123.28(9), C(27)–Nb–N(1) 99.91(10), C(27)–Nb–N(2) 86.65(8), C(27)–Nb–N(3) 113.62(9), Nb–C(23)–Si(1) 131.31(11), Nb–C(27)–Si(2) 119.91(14). $\tau = (\beta - \alpha)/60 = (170.80 - 114.15)/60 = 0.944$.

pyridylmethylanilido ligand and the imido N atom lying on the axis and an equatorial plane consisted of the two alkoxide ligands and the anilido N atom. The axial N(1)–Nb–N(2) bond angle in **3a** [172.21(8)°] is slightly smaller than that in **3b** [173.37(8)°], and the Nb–N(1)–C(1) bond angle in **3a** [177.24(17)°] is larger than that in **3b** [169.53(17)°]. The sums of the equatorial O(1)–Nb–O(2), O(1)–Nb–N(3) and O(2)–Nb–N(3) bond angles in **3a,b** are 351.1, 350.09°, respectively. These indicate that the nitrogen atom in the pyridine is located at trans-position of the imido ligand and that

complexes **3a,b** fold a linear structure from C(1) through N(2). Furthermore, τ -value, one for an ideal trigonal bipyramid and zero for a square-pyramidal coordination [$\tau = (\beta - \alpha)/60$ with α and β being the largest basal angles] is 0.894, 0.924, respectively,¹⁷ suggesting their trigonal bipyramidal structures. The N(1)–Nb–N(3) bond angles in **3a,b** [99.35(9)°, 103.12(8)°, respectively] are larger than the N(2)–Nb–N(3) bond angles [74.92(8)°, 75.38(7)°, respectively]. The Nb–O(1) and Nb–O(2) distances [1.9618(15)–1.9875(17) Å] are shorter than those in $\text{Nb}(\text{N}-2,6\text{-Me}_2\text{C}_6\text{H}_3)(\text{N}=\text{C}^t\text{Bu}_2)[\text{OCH}(\text{CF}_3)_2]_2(\text{HN}=\text{C}^t\text{Bu}_2)$ [1.9879(14), 1.9986(12) Å],^{11j} whereas the Nb–N(1) bond distances [1.7913(19), 1.7899(17) Å for **3a, 3b**, respectively] are close [1.790(2) Å].^{11j}

Figure 2 shows ORTEP drawings for $\text{Nb}(\text{N}-2,6\text{-}i\text{Pr}_2\text{C}_6\text{H}_3)\text{-Me}_2(\text{L})$ (**4b**, different views).¹⁶ The complex also folds a distorted trigonal bipyramidal geometry around niobium ($\tau = 0.967$), as observed in **3a,b**. The axial N(1)–Nb–N(2) bond angle [169.74(10)°] is smaller than that in the alkoxide analogue (**3b**) [173.37(8)°], but the Nb–N(1)–C(1) bond angle [174.2(2)°] is larger than that in **3b** [169.53(17)°]. As observed in **3b**, the N(1)–Nb–N(3) bond angle [96.73(10)°] is larger than the N(2)–Nb–N(3) bond angle [73.00(9)°]. The sum of the equatorial C(19)–Nb–C(19ⁱ), C(19)–Nb–N(3) and C(19ⁱ)–V–N(3) bond angles is 351.53°, clearly suggesting that complex **4b** folds a linear structure from C(1) through N(2). Moreover, as shown in **Figure 2**, the torsion angles in **4b** [N(1)–Nb–N(3)–C(13) (180.0°), N(1)–Nb–N(3)–C(14) (0.0°), N(2)–Nb–N(3)–C(13) (0.0°), N(2)–Nb–N(3)–C(14) (180.0°), N(3)–Nb–N(2)–C(8) (180.0°), and N(3)–Nb–N(2)–C(12) (0.0°)] strongly suggest that the pyridine ligand frame possesses a plane perpendicular to a plane consisting of two methyl groups and niobium atoms as well as two phenyl rings (in the arylimido and anilido ligands). These results clearly indicate that the basic structure in **4b** is similar to that in the vanadium analogue, $\text{V}(\text{N}-1\text{-adamantyl})\text{Me}_2(\text{L})$.^{6e}

Figure 3 shows an ORTEP drawing for $\text{Nb}(\text{N}-2,6\text{-Me}_2\text{C}_6\text{H}_3)\text{-}(\text{CH}_2\text{SiMe}_3)_2(\text{L})$ (**5a**).¹⁶ The complex also folds a distorted trigonal bipyramidal geometry around niobium ($\tau = 0.944$). The axial N(1)–Nb–N(2) bond angle [170.80(7)°] is smaller than that in the alkoxide analogue (**3a**) [172.21(8)°] but is larger

Table 1. Reaction with Ethylene by $\text{Nb}(\text{NAr})\text{Me}_2[2\text{-}(2,6\text{-Me}_2\text{C}_6\text{H}_3)\text{NCH}_2(\text{C}_5\text{H}_4\text{N})]$ [Ar = 2,6-Me₂C₆H₃ (**4a**), 2,6-*i*Pr₂C₆H₃ (**4b**)]–MAO Catalyst Systems (Ethylene 8 atm, in Toluene, 10 min)^a

run	cat./ μmol	Al/Nb ^b	oligomer ^c				PE ^g	
			TON ^d	TOF ^e /h ⁻¹	C ₄ ^f /%	C ₆ ^f /%	TON ^d	wt %
1	4a (3.0)	25	trace					
2	4a (3.0)	50	74	444	96.3	3.7	6	7.4
3	4a (3.0)	100	103	617	96.0	4.0	17	14
4	4a (3.0)	250	112	671	95.8	4.2	59	35 ^h
5	4a (3.0)	250	126	755	94.9	5.1	51	29
6	4a (3.0)	500	trace				trace	
7	4b (1.0)	100	398	2390	95.4	4.6	18	4.3
8	4b (1.0)	250	2960	17 800	94.5	5.5	39	1.3
9	4b (1.0)	250	2810	16 800	94.3	5.7	68	2.4
10	4b (1.0)	500	1250	7480	94.9	5.1	154	11
11	4b (1.0)	1000	570	3420	91.0	9.0	225	28
12	4b (1.0)	2000	354	2120	90.3	9.7	264	43
13	4b (1.0)	3000	175	1050	92.9	7.1	292	63

^aConditions: toluene 30 mL, ethylene 8 atm, 25 °C, 10 min, D-MAO white solid (prepared by removing AlMe₃, toluene from TMAO-S). ^bAl/Nb molar ratio. ^cOligomer = 1-butene + 1-hexene formed. ^dTON = (molar amount of ethylene reacted)/mol-Nb. ^eTOF = TON/h. ^fBy GC analysis vs internal standard. ^gCollected as MeOH–HCl insoluble portion. ^hMelting temperature at 134.1 °C by DSC thermogram.¹⁹

Table 2. Ethylene Dimerization by Nb(N-2,6-*i*-Pr₂C₆H₃)Me₂[2-(2,6-Me₂C₆H₃)NCH₂(C₃H₄N)] (4b)–MAO Catalyst System (Ethylene 8 atm, in Toluene, 10 min): Effects of Temperature, Al/Nb Molar Ratios^a

run	Al/Nb ^b	temp./°C	oligomer ^c				PE ^g	
			TON ^d	TOF ^e /h ⁻¹	C ₄ ^f /%	C ₆ ^f /%	TON ^d	wt %
8	250	25	2960	17 800	94.5	5.5	39	1.3
14	50	50	202	1210	94.0	6.0	18	8.1
15	100	50	2120	12 700	92.6	7.4	75	3.4
16	250	50	3250	19 500	92.5	7.5	160	4.7 ^h
17	250	50	2980	17 900	92.5	7.5	228	7.1
18	50	80	trace				113	
19	100	80	1270	7640	91.6	8.4	121	8.7
20	250	80	2150	12 900	89.2	10.8	296	12
21	250	80	2350	14 100	91.4	8.6	143	5.7
22	500	80	857	5140	89.4	10.6	157	15

^aConditions: complex **4b** 1.0 μmol, toluene 30 mL, ethylene 8 atm, 10 min, D-MAO white solid (prepared by removing AlMe₃, toluene from TMAO-S). ^bAl/Nb molar ratio. ^cOligomer = 1-butene + 1-hexene formed. ^dTON = (molar amount of ethylene reacted)/mol-Nb. ^eTOF = TON/h. ^fBy GC analysis vs internal standard. ^gCollected as MeOH–HCl insoluble portion. ^hMelting temperature at 133.9 °C by DSC thermogram.¹⁹

Table 3. Ethylene Dimerization by Nb(N-2,6-*i*-Pr₂C₆H₃)Me₂[2-(2,6-Me₂C₆H₃)NCH₂(C₃H₄N)] (4b)–MAO Catalyst System: Time Course and Ethylene Pressure Dependence^a

run	ethylene/atm	temp./°C	time/min	oligomer ^b				PE ^f	
				TON ^c	TOF ^d /h ⁻¹	C ₄ ^e /%	C ₆ ^e /%	TON ^c	wt %
23	8	25	5	1500	18 100	95.4	4.6	29	1.9
8	8	25	10	2960	17 800	94.5	5.5	39	1.3
24	8	25	20	4540	13 600	92.1	7.9	171	3.6
25	8	50	5	1770	21 200	93.1	6.9	114	6.1
16	8	50	10	3250	19 500	92.5	7.5	160	4.7
26	8	50	20	5460	16 400	90.3	9.7	214	3.8
27	8	80	5	1310	15 700	93.6	6.4	107	7.6
21	8	80	10	2350	14 100	91.4	8.6	143	5.7
28	8	80	20	2910	8720	86.6	13.4	271	8.5
29	2	25	10	668	4010	96.0	4.0	14	2.1
30	4	25	10	1320	7920	94.9	5.1	57	4.1
31	6	25	10	2190	13 200	93.9	6.1	86	3.8

^aConditions: complex **4b** 1.0 μmol, toluene 30 mL, D-MAO white solid, Al/Nb = 250 (molar ratio). ^bOligomer = 1-butene + 1-hexene formed. ^cTON = (molar amount of ethylene reacted)/mol-Nb. ^dTOF = TON/h. ^eBy GC analysis vs internal standard. ^fCollected as MeOH–HCl insoluble portion.

than that in **4b** [169.74(10)°]. The angle is smaller than that in the vanadium analogue, V(N-2,6-Me₂C₆H₃)(CH₂SiMe₃)₂(L) [**V**, 173.78(5)°].¹⁸ The Nb–N(1)–C(1) bond angle [177.38(16)°] is close to that in **3a** [177.24(17)°] and **V** [176.96(11)°]¹⁸ but is larger than that in **4b** [174.2(2)°]. As also shown in **3a,b** and **4b**, the N(1)–Nb–N(3) bond angle [98.59(9)°] is larger than the N(2)–Nb–N(3) bond angle [72.73(7)°]. The sum of the equatorial C(23)–Nb–C(27), C(23)–Nb–N(3) and C(27)–Nb–N(3) bond angles is 351.05°, clearly suggesting that complex **5a** folds a linear structure from C(1) through N(2). The Nb–C bond distances in **5a** [2.179(3), 2.196(3) Å] are close to those in **4b** [2.195(2) Å] but longer than those in the V–C [2.0758(19), 2.0864(18) Å].¹⁸ The C(23)–Nb–C(27) bond angle in **5a** [114.15(9)°] is larger than the C(19)–Nb–C(19ⁱ) bond angle in **4b** [111.71(9)°], probably because of a steric bulk of SiMe₃ group in **5a** compared with the methyl group in **4b**; the angle in **5a** is also close to the vanadium analogue [114.08(6)].¹⁸

2.2. Reaction with Ethylene by Nb(NAr)Me₂[2-(2,6-Me₂C₆H₃)NCH₂(C₃H₄N)] [Ar = 2,6-Me₂C₆H₃ (4a**), 2,6-*i*-Pr₂C₆H₃ (**4b**), 2-MeC₆H₄ (**4c**)] in the Presence of MAO and Borate.** Reactions with ethylene using the dimethyl complexes, Nb(NAr)Me₂(L) [Ar = 2,6-Me₂C₆H₃ (**4a**),

2,6-*i*-Pr₂C₆H₃ (**4b**), 2-MeC₆H₄ (**4c**)], were conducted in the presence of MAO cocatalyst, according to the similar procedures employed for the vanadium analogues (shown in Scheme 1).⁶ The results in toluene at 25 °C with various Al/Nb molar ratios are summarized in Table 1.¹⁹

It turned out that reactions with ethylene by **4a,b** afforded 1-butene (and 1-hexene) as the major products accompanied by producing linear polyethylene [PE, confirmed by differential scanning calorimetry (DSC) thermogram, melting temperature at 134.1 °C, run 4].¹⁹ In contrast, the activity by **4c** was negligible under the same conditions (as in runs 4, 5 and runs 8, 9, Al/Nb = 250, shown in the Supporting Information).¹⁹ This might be the similar observation in the ethylene polymerization using [NbCl₂(O-2,4-R'₂C₆H₂-6-CH₂)₃N] (R' = Me, ^tBu) that the activity in *n*-octane was much higher than those conducted in toluene.^{20c} The probable reason would be assumed as due to coordination of toluene in the formed active (cationic alkyl) species.^{20,21}

It was revealed that the activities [expressed as turnover number (TON), turnover frequency (TOF)] by **4a,b**–MAO catalyst systems were affected by Al/Nb molar ratios. It seems likely that the percentage of PE especially by **4b** increased with increasing the ratio (runs 7–13):¹⁹ the ratio of 250 (runs 4,5,

and 8,9) seemed to be optimized in terms of the activity and the selectivity of oligomer. The diisopropylphenyl analogue (**4b**) showed higher activity than the dimethylphenyl analogue (**4a**), the major product was 1-butene (94.3–94.5%, runs 8,9), and the results are reproducible (runs 8,9 and the data are shown in the Supporting Information).¹⁹

It should be noted that both the high activity and selectivity of 1-butene are maintained (or became rather high) even if these reactions by **4b** were conducted at 50 °C (runs 16,17, Table 2).¹⁹ This is the noteworthy contrast to that using the vanadium analogues, whereas the activity by the V(NAd)Cl₂(L)–MAO catalyst system extensively decreased at 50 °C.^{6d} The activity by **4b**, however, slightly decreased at 80 °C. The activities at 50 and 80 °C were also affected by the Al/Nb molar ratios, and, as observed in Table 2, the ratio of 250 (runs 16,17, and 20,21) seemed to be optimized in terms of both the activity and selectivity. It seems likely that amount of PE byproduced increased at high temperature, probably because of partial decomposition of the catalytically active species and/or partial ligand dissociation (probably leading formation of another active species) assumed previously in the vanadium catalyst systems.^{6a,c,19}

Table 3 summarizes results in the time course dependences at 25, 50, and 80 °C, and the ethylene pressure dependence (at 25 °C) toward both the activity and selectivity in the ethylene dimerization using the **4b**–MAO catalyst system.¹⁹ Figure 4 also

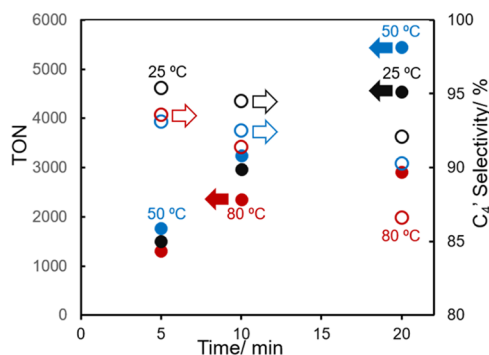


Figure 4. Time course in ethylene dimerization by Nb(N-2,6-*i*-Pr₂C₆H₃)Me₂[2-(2,6-Me₂C₆H₃)NCH₂(C₅H₄N)] (**4b**)–MAO catalyst system (ethylene 8 atm): temperature dependence toward TONs (filled circle) and C₄ selectivity (circle in plain). Detailed data are shown in Table 3.

shows the time course dependences toward the TONs and the selectivity of 1-butene, and the selectivity decreased over time course, suggesting that, as observed in the reaction using the vanadium analogues,^{6b,d} the initial products in the reaction was 1-butene and 1-hexene was formed by the subsequent reaction of ethylene with 1-butene accumulated in the reaction mixture. Importantly, degree of decrease in the selectivity of 1-butene after 20 min was affected by the reaction temperature; the selectivity decreased rapidly at 80 °C (runs 21, 27, 28) compared with those conducted at 25, 50 °C (runs 8, 16, 23–26).¹⁹ It should be noted that the activities (expressed as TONs and TOFs) conducted at 50 °C were higher than those conducted at 25 °C; the decrease in the activity over time course at 80 °C was rather significant, suggesting a possibility of the catalyst deactivation.¹⁹

As shown in Figure 5, a first-order relationship between TOF value and the ethylene pressures was observed (runs 8, 29–31, Table 3). It has been known that the ethylene oligomerization

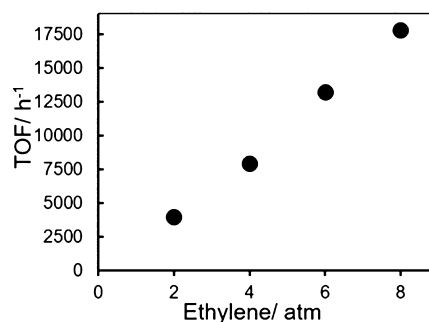


Figure 5. Ethylene pressure dependence in ethylene dimerization by Nb(N-2,6-*i*-Pr₂C₆H₃)Me₂[2-(2,6-Me₂C₆H₃)NCH₂(C₅H₄N)] (**4b**)–MAO catalyst system (25 °C). Detailed data are shown in Table 3.

proceeds via a metal-hydride (metal-alkyl) or metallacycle intermediate, and the ethylene pressure dependence toward the activity is different in these pathways.^{2d,6b} Therefore, the result (first-order dependence) could suggest that the metal-hydride (or metal-alkyl) species play a role in this catalysis.

It should be noted that, as shown in Table 4, significant increases in the activities were observed in ethylene dimerization by **4a,b**–MAO catalyst systems by addition of [Ph₃C][B(C₆F₅)₄] (borate) as the cocatalyst.¹⁹ The activity by **4a**–MAO catalyst system increased upon addition of 1.5 equiv of [Ph₃C][B(C₆F₅)₄] [TOF = 31 700 h⁻¹ (run 32) vs 755 (run 5), at 25 °C]; the activity increased at 50 °C (run 33). Remarkable increase in the activity by addition of the borate was also observed in the ethylene dimerization by **4b**–MAO catalyst system [ex. TOF = 19 500 h⁻¹ (run 16) vs 650 000 h⁻¹ (run 37, Al/Nb = 100)], and the selectivity of oligomers also increased in the presence of MAO and borate cocatalysts [ex. percentage of PE byproduced = 4.7 wt % (run 16) vs 1.0 wt % (run 37)]. The reaction did not take place when only borate was added in the solution without MAO (run 34), suggesting that both MAO and borate are necessary in this catalysis. The activity in the presence of Al^{*i*}Bu₃ and borate cocatalysts (run 35) was the same level as that in the presence of MAO (run 16), and the selectivity of 1-butene was apparently low (63.1%, run 35). It was also revealed that the activity was affected by the Nb/Al molar ratios (runs 36–40, runs 41, 42, 45, 46),¹⁹ and as observed in Table 1, the percentage of PE byproduced increased high Nb/Al molar ratios (runs 39, 40, and 46).¹⁹ The resultant PEs byproduced were ethylene oligomers containing terminal olefinic double bonds (confirmed by ¹H NMR spectrum as well as DSC thermograms).¹⁹

Moreover, the activity under low catalyst concentration conditions (**4b** 0.5 μmol) increased upon further addition of borate (3.0 equiv).¹⁹ It should be noteworthy that under optimized conditions with low **4b** concentration conditions at 50 °C, TON of 234 000 (TOF 1 400 000 h⁻¹) could be attained after 10 min (run 43), and the TOF at the initial stage (after 5 min) was 2 100 000 h⁻¹ (583 s⁻¹), which is the same level as that by the vanadium analogue, V(NAd)Cl₂(L)–MAO catalyst system, conducted at 25 °C (508 s⁻¹).^{6d} Because the selectivity of 1-butene decreased over time course (runs 43, 44), this also suggests that 1-hexene was formed by the subsequent reaction of ethylene with 1-butene accumulated in the reaction mixture. Although the observed selectivity of 1-butene seems rather low, the **4b**–MAO and [Ph₃C][B(C₆F₅)₄] (borate) catalyst system showed the highest activity for ethylene dimerization at 50 °C with minimizing of the byproduction of PE.

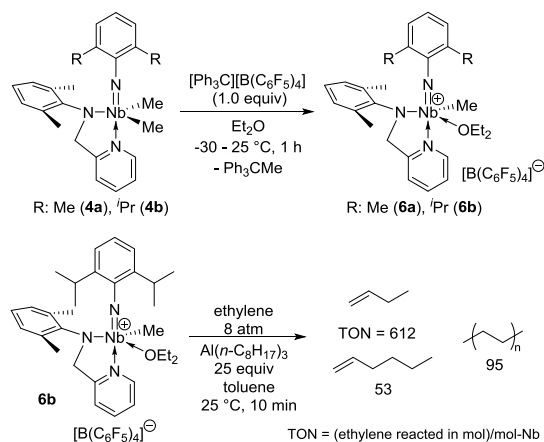
Table 4. Ethylene Dimerization by Nb(NAr)Me₂[2-(2,6-Me₂C₆H₃)NCH₂(C₅H₄N)] [Ar = 2,6-Me₂C₆H₃ (4a), 2,6-*i*-Pr₂C₆H₃ (4b)]–MAO, [Ph₃C][B(C₆F₅)₄] (B) Catalyst System (Ethylene 8 atm, 10 min)^a

run	cat.	cocat.	Al/B/Nb ^b	temp/°C	oligomer ^c				PE ^g	
					TON ^d	TOF ^e /h ⁻¹	C ₄ ^f %	C ₆ ^f %	TON ^d	wt %
5	4a (3.0)	MAO	250	25	126	755	94.9	5.1	51	29
32	4a (1.0)	MAO/B	250/1.5	25	5280	31 700	90.9	9.1	328	5.9
33	4a (1.0)	MAO/B	250/1.5	50	5650	33 900	80.1	19.9	428	7
34	4b (1.0)	B	1.5	50	trace				trace	
16	4b (1.0)	MAO	250	50	3250	19 500	92.5	7.5	160	4.7
35	4b (1.0)	Al ⁱ Bu ₃ /B	100/1.5	50	3460	20 800	63.1	17.3	310	8.2
36	4b (1.0)	MAO/B	50/1.5	50	73 100	439 000	77.6	20.0	228	0.3
37	4b (1.0)	MAO/B	100/1.5	50	108 000	650 000	77.0	20.3	1080	1.0
38	4b (1.0)	MAO/B	200/1.5	50	42 900	257 000	90.7	7.6	727	1.7
39	4b (1.0)	MAO/B	250/1.5	50	19 500	117 000	88.7	11.3	677	3.4
40	4b (1.0)	MAO/B	400/1.5	50	4920	29 500	89.2	10.8	913	16
41	4b (0.5)	MAO/B	100/1.5	50	10 700	64 300	89.9	10.1	349	3.2
42	4b (0.5)	MAO/B	200/1.5	50	178 000	1 070 000	79.3	18.4	884	0.5
43	4b (0.5)	MAO/B	200/3.0	50	234 000	1 400 000	80.5	17.5	656	0.3
44 ^h	4b (0.5)	MAO/B	200/3.0	50	175 000	2 100 000	84.4	14.1	328	0.2
45	4b (0.5)	MAO/B	300/1.5	50	117 000	700 000	83.0	15.4	863	0.7
46	4b (0.5)	MAO/B	400/1.5	50	20 000	112 000	89.2	10.8	1070	5.1

^aConditions: toluene 30 mL, ethylene 8 atm, 25 °C, 10 min, D-MAO white solid. ^bAl/B/Nb molar ratio, B = [Ph₃C][B(C₆F₅)₄]. ^cOligomer = 1-butene + 1-hexene formed. ^dTON = (molar amount of ethylene reacted)/mol-Nb. ^eTOF = TON/h. ^fBy GC analysis vs internal standard. ^gCollected as MeOH–HCl insoluble portion. ^hTime 5 min.

2.3. Reaction of Nb(NAr)Me₂[2-(2,6-Me₂C₆H₃)NCH₂(C₅H₄N)] [Ar = 2,6-Me₂C₆H₃ (4a), 2,6-*i*-Pr₂C₆H₃ (4b)] with [Ph₃C][B(C₆F₅)₄] and the Reaction with Ethylene. To obtain further information concerning the assumed catalytically active species, reaction of the dimethyl complex (4a) with 1.0 equiv of [Ph₃C][B(C₆F₅)₄] was conducted in Et₂O (Scheme 4).¹⁴ After removal of volatiles in the mixture, the resultant oil

Scheme 4. Synthesis of [Nb(NAr)Me(Et₂O)_n{2-(2,6-Me₂C₆H₃)NCH₂(C₅H₄N)}]⁺ [Ar = 2,6-Me₂C₆H₃ (6a), 2,6-*i*-Pr₂C₆H₃ (6b)] from Nb(NAr)Me₂[2-(2,6-Me₂C₆H₃)NCH₂(C₅H₄N)] (4a,b) by Treating with 1.0 equiv of [Ph₃C][B(C₆F₅)₄] in Et₂O, and Reaction of Ethylene with 6b in the Presence of Al(*n*-C₈H₁₇)₃



was washed with *n*-hexane and was dried in vacuo. A resonance ascribed to niobium–methyl protons (1.35 ppm), which is different from that in 4a (0.56 ppm), was observed in the ¹H NMR spectrum (in CDCl₃ at 25 °C, Figure 6b,c), and resonance ascribed to methylene protons (N–CH₂–py) became two doublet and two resonances ascribed to methyl protons

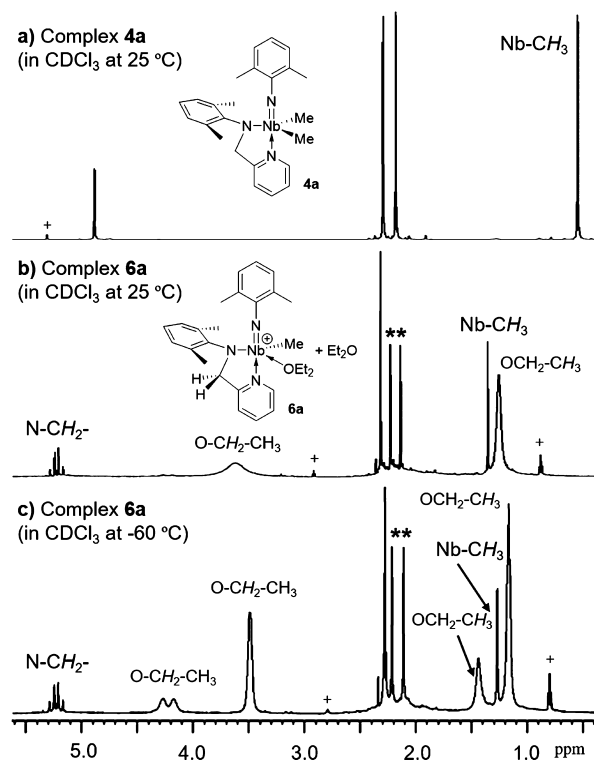


Figure 6. ¹H NMR spectra (in CDCl₃) for (a) Nb(N-2,6-Me₂C₆H₃)Me₂[2-(2,6-Me₂C₆H₃)NCH₂(C₅H₄N)] (4a) and (b,c) [Nb(N-2,6-Me₂C₆H₃)Me(Et₂O)_n{2-(2,6-Me₂C₆H₃)NCH₂(C₅H₄N)}]⁺ (6a) prepared from 4a by treating with [Ph₃C][B(C₆F₅)₄] in Et₂O. Resonances marked with + are impurities.

connected to anilide ligand (in high certainty) were observed (marked with * in Figure 6b,c). Most of all resonances observed in the ¹H NMR spectra, shown in Figure 6b,c, were thus assigned to protons of an assumed cationic complex. Moreover, resonances ascribed to protons in Ph₃C(CH₃) (ca. 2.3 ppm)

in the ^1H NMR spectrum (in CDCl_3),²² and three resonances ascribed to C_6F_5 group were also observed in the ^{19}F NMR spectrum.¹⁴ The similar reaction in toluene- d_8 afforded two separated solution consisting of toluene soluble portion (clear pale brown) and toluene insoluble deep brown tan residue at the bottom. This is a similar observation in the reaction of $\text{V}(\text{NAd})\text{Me}_2(\text{L})$ with $[\text{Ph}_3\text{C}][\text{B}(\text{C}_6\text{F}_5)_4]^{6e}$ and $\text{Cp}^*\text{TiMe}_2(\text{O}-2,6\text{-}^i\text{Pr}_2\text{C}_6\text{H}_3)$ ^{23c} and the others,²³ strongly suggesting formation of cationic methyl species. Moreover, on the basis of integration ratio in the ^1H NMR spectra (Figure 6b), 2 equiv of Et_2O molecules, that seemed to be difficult to remove in vacuo, were contained in **6a**. The VT-NMR spectra showed that a broad resonances ascribed to Et_2O at 25 °C became two sets at -60 °C: one Et_2O was coordinated to the niobium and free Et_2O , suggesting an existence of the fast exchange (coordination and dissociation of Et_2O , Figure 6b,c) in the solution. Therefore, the formula of the isolated cationic complex could be expressed as $[\text{Nb}(\text{N}-2,6\text{-Me}_2\text{C}_6\text{H}_3)\text{Me}(\text{L})]^+[\text{B}(\text{C}_6\text{F}_5)_4]^- (\text{Et}_2\text{O})_2$ (**6a**) in high certainty. Similarly, the treatment of $\text{Nb}(\text{N}-2,6\text{-}^i\text{Pr}_2\text{C}_6\text{H}_3)\text{-Me}_2(\text{L})$ (**4b**) with $[\text{Ph}_3\text{C}][\text{B}(\text{C}_6\text{F}_5)_4]$ in Et_2O yielded $[\text{Nb}(\text{N}-2,6\text{-}^i\text{Pr}_2\text{C}_6\text{H}_3)\text{Me}(\text{L})]^+[\text{B}(\text{C}_6\text{F}_5)_4]^- (\text{Et}_2\text{O})_2$ (**6b**).¹⁴

Importantly, the cationic methyl complex **6b** afforded 1-butene, 1-hexene, and PE without MAO [Scheme 4, in the presence of $\text{Al}(n\text{-C}_8\text{H}_{17})_3$, which should be the weak reagent for alkylation and/or chain transfer and plays a role as scavenger as well as for removal of coordinated Et_2O].^{23g,h,24} The result thus strongly suggests that the cationic methyl complex plays a role in this catalysis.^{25,26}

2.4. Solution Phase XANES Analysis of Catalyst Solution Containing Nb(NAr)Me₂(L) in the Presence of MAO Cocatalyst: Exploring the Oxidation State of the Catalytically Active Species in the Ethylene Dimerization. On the basis of the first-order relationship between the activity and ethylene pressure (Table 3 and Figure 5), isolation of the stable cationic complexes, $[\text{Nb}(\text{NAr})\text{Me}(\text{L})]^+[\text{B}(\text{C}_6\text{F}_5)_4]^- (\text{Et}_2\text{O})_2$ (**6a,b**), and reaction of **6b** with ethylene to afford 1-butene (Scheme 4), it is highly suggested that the cationic alkyl complex plays a role in this catalysis of ethylene dimerization using $\text{Nb}(\text{NAr})\text{Me}_2(\text{L})$ (**4a,b**)-cocatalyst systems. Synchrotron XAS of the catalyst solution has also been chosen in this study, as conducted previously in the vanadium catalysis,²⁷ because the method (Nb K edge analysis, 18.98 keV, through the use of synchrotron radiation at SPring-8, BL01B1 beamline) enables us obtainment of the information concerning oxidation state and the basic structure (by Nb K pre-edge and edge peaks in XANES analysis, XANES = X-ray absorption near edge structure) in the catalyst solution.^{27–30}

Figure 7 shows Nb K-edge XANES spectra of toluene solution containing the dimethyl complexes (**4a,b**) and the spectra of **4b** in the presence of MAO (10, 50 equiv) at 25 °C (Nb 50 $\mu\text{mol}/\text{mL}$). The XANES spectra of **4a** and **4b** show pre-edge peaks at 18 974.7 and 18 975.3 eV, respectively, which have been ascribed to a transition from 1s to 3d + 4p.^{29,30} Note that, no significant differences in the pre-edge peak positions and intensities in the pre-edge peaks from those in **4b** were observed upon addition of MAO [18 974.7 eV upon addition of 10 and 50 equiv of MAO, Figure 7]. Also note that the XANES spectra (edge region in addition of pre-edge) of **4b** in the presence of MAO (10 and 50 equiv) are very close to that in the homogeneous toluene solution containing the dimethyl complex (**4b**). Therefore, the results strongly suggest in high certainty that both the oxidation states and the basic structures

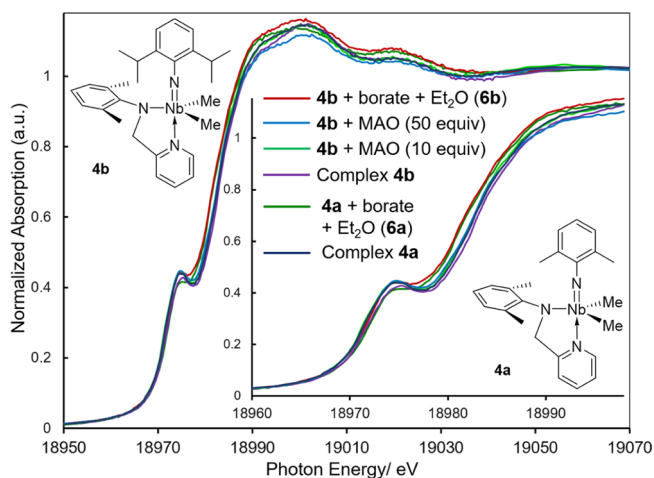


Figure 7. The solution-phase Nb K-edge XANES spectra (in toluene at 25 °C) for $\text{Nb}(\text{NAr})\text{Me}_2[2\text{-}(2,6\text{-Me}_2\text{C}_6\text{H}_3)\text{NCH}_2(\text{C}_5\text{H}_4\text{N})]$ [Ar = 2,6-Me₂C₆H₃ (**4a**), 2,6-ⁱPr₂C₆H₃ (**4b**)], and the spectra for **4b** in the presence of MAO (10, 50 equiv). The Nb K-edge XANES spectra (in Et_2O at 25 °C) for **4a,b** upon addition of 1.0 equiv of $[\text{Ph}_3\text{C}][\text{B}(\text{C}_6\text{F}_5)_4]$ (borate).

are maintained upon addition of MAO in these catalyst solutions consisting of **4b** and MAO.

Moreover, no significant changes in the spectra in the edge region were observed when **4a** and **4b** was added 1.0 equiv of $[\text{Ph}_3\text{C}][\text{B}(\text{C}_6\text{F}_5)_4]$ (borate) in Et_2O (formation of **6a,b** according to Scheme 4), whereas slightly shifts (ca. 0.3 eV) in the pre-edge peaks were observed [18 975.0 (**4a** and borate, **6a**), 18 974.7 (**4b** and borate, **6b**)]. These also strongly suggest in high certainty that both the oxidation states and the basic structures are maintained upon addition of borate.

3. CONCLUDING REMARKS

The experimental results observed through this study can be summarized as follows.

- (1) (Arylimido)niobium(V) complexes containing 2-pyridylmethylamido ligands, $\text{Nb}(\text{NAr})\text{X}_2(\text{L})$ [L = 2-(2,6-Me₂C₆H₃)NCH₂(C₅H₄N); X = NMe₂ (**2a,b**), OCH(CF₃)₂ (**3a–c**), Me (**4a–c**), CH₂SiMe₃ (**5a**); Ar = 2,6-Me₂C₆H₃ (**a**), 2,6-ⁱPr₂C₆H₃ (**b**), 2-MeC₆H₄ (**c**)] have been prepared and identified.¹⁴ Structures of **3a,b**, **4b**, and **5a** were determined by X-ray crystallography.¹⁶ In particular, the dimethyl complexes (**4a–c**) were prepared from the bis(alkoxo) analogues (**3a–c**) by reaction with MeMgBr.
- (2) Two dimethyl complexes (**4a,b**) exhibited from moderate and high catalytic activities for ethylene dimerization in the presence of MAO, whereas the activity by **4c** was negligible under the same conditions.¹⁷ The activity by **4b** was higher than that by **4a**, indicating that a steric bulk in the arylimido ligand play a role in this catalysis. This is an interesting contrast to that in the related (imido) vanadium complex catalysts (shown in Scheme 1),^{6a,c} in which the dimethylphenylimido analogue, $\text{V}(\text{N}-2,6\text{-Me}_2\text{C}_6\text{H}_3)\text{Cl}_2(\text{L})$, afforded PE^{6a} and both the phenylimido and *o*-tolylimido analogues showed notable catalytic activity for the selective ethylene dimerization.^{6a,c}

The activity by **4b** at 50 °C was higher than those conducted at 25 and 80 °C, whereas significant decrease in the activity was

observed by the vanadium analogue, $V(\text{NAD})\text{Cl}_2(\text{L})$, at 50 °C.^{6d} The major product was 1-butene, and 1-hexene was formed by subsequent reaction of ethylene with 1-butene accumulated in the reaction mixture. A first-order relationship between the activity (TOF) and ethylene pressure was observed, suggesting that the metal-alkyl species (via coordination, insertion, and β -hydrogen elimination pathway) would play a role in this catalysis.

- (3) Significant increases in the activities by **4a,b** have been attained upon further addition of $[\text{Ph}_3\text{C}][\text{B}(\text{C}_6\text{F}_5)_4]$. Under optimized conditions with low **4b** concentration conditions at 50 °C, TON of 234 000 (TOF 1 400 000 h^{-1}) has been attained after 10 min (run 43, Table 4), and the TOF at the initial stage (after 5 min) was 2 100 000 h^{-1} (583 s^{-1}), which is the same level as that by the vanadium analogue, $V(\text{NAD})\text{Cl}_2(\text{L})$ –MAO catalyst system, conducted at 25 °C (508 s^{-1}).^{6d}
- (4) Reactions of the dimethyl complexes (**4a,b**) with 1.0 equiv of $[\text{Ph}_3\text{C}][\text{B}(\text{C}_6\text{F}_5)_4]$ in Et_2O afforded the cationic complexes, $[\text{Nb}(\text{NAr})\text{Me}(\text{L})]^+[\text{B}(\text{C}_6\text{F}_5)_4]^- (\text{Et}_2\text{O})_2$ (**6a,b**). The reaction of **6b** with ethylene afforded 1-butene and 1-hexene even in the absence of MAO, clearly suggesting that the cationic complex plays a role as the catalytically active species.
- (5) XANES spectra of the catalyst solutions containing **4b** (in toluene at 25 °C) and MAO (10 and 50 equiv) showed no significant differences in the pre-edge peak positions and the intensities from that in the dimethyl complex (**4b**). The results thus strongly suggest that the oxidation states and basic structures are maintained upon addition of MAO in the catalyst solutions consisting of **4b** and MAO.

Taking into account the above facts, it is demonstrated in high certainty that the cationic niobium(V)-alkyl species play a role in this catalysis, and a nature of the catalytically active species (steric bulk of the arylimido ligand) directly affects the reactivity. As far as we know, this is the first demonstration of homogeneous niobium complex catalysts that exhibit remarkable catalytic activity for ethylene dimerization even at 50 °C. At this stage, we have not yet had clear explanation concerning the difference between the vanadium and niobium analogues in terms of activity, thermal stability, selectivity (byproduction of PE in the niobium systems), and so forth. We however highly believe the information should be potentially important for designing efficient molecular catalysis with niobium for precise olefin polymerization, oligomerization.

4. EXPERIMENTAL SECTION

4.1. General Procedure. All experiments were carried out under a nitrogen atmosphere in a Vacuum Atmospheres drybox. Anhydrous grade toluene, *n*-hexane, diethyl ether, and dichloromethane (Kanto Kagaku Co., Ltd.) were transferred into a bottle containing molecular sieves (a mixture of 3A 1/16, 4A 1/8, and 13X 1/16) in the drybox under nitrogen stream and were passed through an alumina short column under N_2 stream prior to use. $\text{Nb}(\text{NMe}_2)_5$ (Strem Chemicals, Inc.) was used as received, and $\text{Nb}(\text{N-2,6-}i\text{-Pr}_2\text{C}_6\text{H}_3)(\text{NMe}_2)_3$ was prepared according to the reported procedure.^{11c} Reagents such as $(\text{CF}_3)_2\text{CHOH}$ (TCI Co., Ltd.), MeMgBr (3.0 M in diethyl ether, Aldrich Chemical Co.), and $\text{Me}_3\text{SiCH}_2\text{MgCl}$ (1.0 M in diethyl ether, Aldrich Chemical Co.) were used as received. Polymerization grade ethylene (purity > 99.9%, Sumitomo Seika Co. Ltd.) was used as received. Toluene and AlMe_3 in the commercially available MAO [T-MAO, 9.5 wt % (Al) toluene solution, Tosoh Finechem Co.] were removed under reduced pressure (at ca. 50 °C for removing toluene,

AlMe_3 , and then heated at >100 °C for 1 h from completion) in the drybox to give white solids.⁶

Elemental analyses were performed by using an EAI CE-440 CHN/O/S elemental analyzer (Exeter Analytical, Inc.). All ^1H , ^{13}C , and ^{19}F NMR spectra were recorded on a Bruker AV500 spectrometer (500.13 MHz for ^1H , 125.77 MHz for ^{13}C). All spectra were obtained in the solvent indicated at 25 °C unless otherwise noted. Chemical shifts are given in ppm and are referenced to SiMe_4 (δ 0.00 ppm, ^1H , ^{13}C) and CFCl_3 (δ 0.00 ppm, ^{19}F), and the coupling constants are given in hertz. GC analysis was performed with a SHIMADZU GC-17A gas chromatograph (Shimadzu Co. Ltd.) equipped with a flame ionization detector.

4.2. Synthesis of $\text{Nb}(\text{N-2,6-Me}_2\text{C}_6\text{H}_3)(\text{NMe}_2)_2[2-(2,6-\text{Me}_2\text{C}_6\text{H}_3)\text{NCH}_2(\text{C}_5\text{H}_4\text{N})]$ (2a**).**
4.2.1. Synthesis of $\text{Nb}(\text{N-2,6-Me}_2\text{C}_6\text{H}_3)(\text{NMe}_2)_3$ (1a**).** Into a toluene solution (30 mL) containing $\text{Nb}(\text{NMe}_2)_5$ (988 mg, 3.19 mmol) was added toluene solution (12 mL) containing 2,6-dimethylaniline (386 mg, 3.19 mmol) at -78 °C. The mixture was stirred at -78 °C for 30 min, and the solution was warmed slowly to room temperature over 2 h. The mixture was then heated slowly to 70 °C over 2 h, and the solution was stirred at 80 °C for 1 h and at 90 °C for 1 h for completion. The reaction mixture was then placed in a rotary evaporator to remove the volatiles. The resultant oil was dissolved in *n*-hexane and the solution was passed through a celite pad, and the filtercake was washed with *n*-hexane. The combined filtrate and wash were placed in a rotary evaporator to remove the volatiles, and the resultant brown oil was confirmed as tris(dimethylamido) complex, $\text{Nb}(\text{N-2,6-Me}_2\text{C}_6\text{H}_3)(\text{NMe}_2)_3$ (**1a**) (1038 mg), confirmed by ^1H NMR spectra (resonances assigned as formation of the desired complex). ^1H NMR (C_6D_6): δ 7.11 (d, 2H, $J = 7.35$ Hz, Ar-H), 6.87 (t, 1H, $J = 7.45$ Hz, Ar-H), 3.11 (s, 18H, $\text{N}(\text{CH}_3)_2$), 2.62 (s, 6H, Ar- CH_3). The resultant sample was used for the next reaction without further purification.

4.2.2. Synthesis of $\text{Nb}(\text{N-2,6-Me}_2\text{C}_6\text{H}_3)(\text{NMe}_2)_2[2-(2,6-\text{Me}_2\text{C}_6\text{H}_3)\text{-NCH}_2(\text{C}_5\text{H}_4\text{N})]$ (2a**).** Into a *n*-hexane solution (80 mL) containing $\text{Nb}(\text{N-2,6-Me}_2\text{C}_6\text{H}_3)(\text{NMe}_2)_3$ (**1a**, 1038 mg, 3.015 mmol) was added a *n*-hexane solution (8 mL) containing 2-(2,6-Me₂C₆H₃)N(H)-CH₂(C₅H₄N) (600 mg, 2.83 mmol) at -30 °C. The reaction mixture was warmed slowly to room temperature, and the mixture was then stirred overnight. The solution was passed through a celite pad, and the filtercake was washed with *n*-hexane. The combined filtrate and wash were placed in a rotary evaporator to remove the volatiles. The resultant oil was dissolved in a minimum amount of toluene and was layered with *n*-hexane. The chilled solution placed in the freezer (-30 °C) afforded yellow microcrystals of **2a**, and the concentrated mother liquor layered with *n*-hexane placed in the freezer (-30 °C) afforded the second crop. Yield: 52.2% (total 850 mg, 1.66 mmol). ^1H NMR (CDCl_3): δ 8.51 (d, 1H, $J = 5.35$ Hz, Ar-H), 7.80 (t, 1H, $J = 7.65$ Hz, Ar-H), 7.41 (d, 1H, $J = 7.90$ Hz, Ar-H), 7.26 (t, 1H, $J = 6.40$ Hz, Ar-H), 7.10 (d, 2H, $J = 7.40$ Hz, Ar-H), 6.91 (q, 3H, $J = 6.70$ Hz, Ar-H), 6.65 (t, 1H, $J = 7.43$ Hz, Ar-H), 4.87 (s, 2H, NCH_2), 3.17 (br s, 6H, $\text{N}(\text{CH}_3)_2$), 2.78 (br s, 6H, $\text{N}(\text{CH}_3)_2$), 2.40 (s, 6H, Ar- CH_3), 2.16 (s, 6H, Ar- CH_3). $^{13}\text{C}\{^1\text{H}\}$ NMR (CDCl_3): δ 163.4, 155.3, 153.5, 149.1, 137.4, 134.6, 131.7, 127.8, 127.1, 123.1, 121.7, 121.1, 120.2, 63.7, 47.3, 18.7. Anal. Calcd for $\text{C}_{26}\text{H}_{36}\text{N}_3\text{Nb}$ (+0.5x toluene): C, 63.54; H, 7.23; N, 12.56. Found: C, 63.23; H, 7.22; N, 12.28.

4.3. Synthesis of $\text{Nb}(\text{N-2,6-}i\text{-Pr}_2\text{C}_6\text{H}_3)(\text{NMe}_2)_2[2-(2,6-\text{Me}_2\text{C}_6\text{H}_3)\text{-NCH}_2(\text{C}_5\text{H}_4\text{N})]$ (2b**).** Into a *n*-hexane solution (60 mL) containing $\text{Nb}(\text{N-2,6-}i\text{-Pr}_2\text{C}_6\text{H}_3)(\text{NMe}_2)_3$ (**1b**, 700 mg, 1.75 mmol) was added a *n*-hexane solution (20 mL) containing 2-(2,6-Me₂C₆H₃)N(H)-CH₂(C₅H₄N) (373 mg, 1.75 mmol) at -30 °C. The reaction mixture was warmed slowly to room temperature, and the mixture was then stirred overnight. The solution was passed through a celite pad, and the filtercake was washed with *n*-hexane. The combined filtrate and wash were placed in a rotary evaporator to remove the volatiles. The resultant oil was dissolved in a minimum amount of toluene and was layered with *n*-hexane. The chilled solution placed in the freezer (-30 °C) afforded yellow microcrystals of **2b** (662 mg, 1.17 mmol). Yield: 66.7%. ^1H NMR (C_6D_6): δ 8.24 (d, 1H, $J = 5.35$ Hz, Ar-H), 7.12 (d, 4H, $J = 7.60$ Hz, Ar-H), 6.97 (m, 2H, Ar-H), 6.81 (td, 1H, $J = 1.52$ and 7.68 Hz, Ar-H), 6.57 (d, 1H, $J = 7.90$ Hz, Ar-H), 6.36 (t, 1H, $J = 6.40$ Hz, Ar-H),

4.70 (d, 1H, $J = 20.5$ Hz, NCH_2), 4.39 (d, 1H, $J = 20.5$ Hz, NCH_2), 4.23 (sep, 2H, $J = 6.86$ Hz, $\text{CH}(\text{CH}_3)_2$), 3.21 (s, 6H, $\text{N}(\text{CH}_3)_2$), 2.95 (s, 6H, $\text{N}(\text{CH}_3)_2$), 2.50 (s, 3H, Ar-CH_3), 2.34 (s, 3H, Ar-CH_3), 1.38 (d, 6H, $J = 5.90$ Hz, $\text{CH}(\text{CH}_3)_2$), 0.92 (d, 6H, $J = 5.80$ Hz, $\text{CH}(\text{CH}_3)_2$). $^{13}\text{C}\{^1\text{H}\}$ NMR (C_6D_6): δ 163.2, 153.7, 152.4, 149.0, 143.1, 136.9, 135.3, 134.3, 123.7, 122.6, 122.4, 121.8, 120.8, 63.7, 48.1, 46.8, 27.8, 24.9, 24.4, 19.5, 18.7. Anal. Calcd for $\text{C}_{30}\text{H}_{44}\text{N}_3\text{Nb}$: C, 63.48; H, 7.81; N, 12.34. Found: C, 63.76; H, 7.96; N, 12.04.

4.4. Synthesis of Nb(N-2,6-Me₂C₆H₃)[OCH(CF₃)₂]₂[2-(2,6-Me₂C₆H₃)NCH₂(C₅H₄N)] (3a). Into a toluene solution (25 mL) containing Nb(N-2,6-Me₂C₆H₃)(NMe₂)₂[2-(2,6-Me₂C₆H₃)-NCH₂(C₅H₄N)] (2a, 279 mg, 0.545 mmol) was added a toluene solution (6 mL) containing (CF₃)₂CHOH (182 mg, 1.09 mmol) slowly at -30 °C. The reaction mixture was warmed slowly to room temperature, and the mixture was then stirred for 3 h. The solution was passed through a celite pad, and the filtercake was washed with toluene. The combined filtrate and wash were placed in a rotary evaporator to remove the volatiles. The resultant oil was dissolved in a minimum amount of toluene and was layered with *n*-hexane. The chilled solution placed in the freezer (-30 °C) afforded white-yellow microcrystals (352 mg, 0.464 mmol). Yield: 85.2%. ^1H NMR (C_6D_6): δ 8.56 (d, 1H, $J = 5.30$ Hz, *Ar-H*), 6.83 (d, 2H, $J = 7.40$ Hz, *Ar-H*), 6.77 (t, 2H, $J = 7.13$ Hz, *Ar-H*), 6.72 (d, 2H, $J = 7.50$ Hz, *Ar-H*), 6.61 (t, 1H, $J = 7.48$ Hz, *Ar-H*), 6.47 (t, 1H, $J = 6.48$ Hz, *Ar-H*), 6.33 (d, 1H, $J = 7.90$ Hz, *Ar-H*), 5.17 (sep, 2H, $J = 5.84$ Hz, $\text{CH}(\text{CF}_3)_2$), 4.32 (s, 2H, NCH_2), 2.25 (s, 6H, *Ar-CH}_3*), 2.23 (s, 6H, *Ar-CH}_3*). $^{13}\text{C}\{^1\text{H}\}$ NMR (C_6D_6): δ 159.9, 156.1, 152.1, 147.1, 138.5, 135.0, 131.6, 128.8, 127.5, 125.4, 124.6, 122.9 (q, $^1J_{\text{CF}} = 283.6$ Hz), 122.78 (q, $^1J_{\text{CF}} = 285.5$ Hz), 122.76, 120.4, 80.0 (sep, $^2J_{\text{CF}} = 32.6$ Hz), 64.1, 18.6, 18.0. ^{19}F NMR (C_6D_6): δ -75.96 (d, $^2J_{\text{FF}} = 6.87$ Hz), -76.23 (d, $^2J_{\text{FF}} = 5.65$ Hz). Anal. Calcd for $\text{C}_{28}\text{H}_{26}\text{F}_{12}\text{N}_3\text{NbO}_2$: C, 44.40; H, 3.46; N, 5.55. Found: C, 44.35; H, 3.45; N, 5.52.

4.5. Synthesis of Nb(N-2,6-Pr₂C₆H₃)[OCH(CF₃)₂]₂[2-(2,6-Me₂C₆H₃)NCH₂(C₅H₄N)] (3b). Into a toluene solution (20 mL) containing Nb(N-2,6-Pr₂C₆H₃)(NMe₂)₂[2-(2,6-Me₂C₆H₃)-NCH₂(C₅H₄N)] (2b, 200 mg, 0.352 mmol) was added a toluene solution (10 mL) containing (CF₃)₂CHOH (118 mg, 0.705 mmol) slowly at -30 °C. The reaction mixture was warmed slowly to room temperature, and the mixture was then stirred for 3 h. The solution was passed through a celite pad, and the filtercake was washed with toluene. The combined filtrate and wash were placed in a rotary evaporator to remove the volatiles. The resultant oil was dissolved in a minimum amount of toluene and was layered with *n*-hexane. The chilled solution placed in the freezer (-30 °C) afforded white-yellow microcrystals (223 mg, 0.274 mmol). Yield: 77.8%. ^1H NMR (C_6D_6): δ 8.57 (d, 1H, $J = 5.35$ Hz, *Ar-H*), 6.87 (d, 2H, $J = 7.45$ Hz, *Ar-H*), 6.83 (d, 2H, $J = 7.50$ Hz, *Ar-H*), 6.81–6.70 (m, 3H, *Ar-H*), 6.45 (t, 1H, $J = 6.40$ Hz, *Ar-H*), 6.32 (d, 1H, $J = 7.95$ Hz, *Ar-H*), 5.19 (sep, 2H, $J = 5.95$ Hz, $\text{CH}(\text{CF}_3)_2$), 4.28 (s, 2H, NCH_2), 3.80 (sep, 2H, $J = 6.79$ Hz, $\text{CH}(\text{CH}_3)_2$), 2.27 (s, 6H, *Ar-CH}_3*), 1.21 (d, 12H, $J = 6.80$ Hz, $\text{CH}(\text{CH}_3)_2$). $^{13}\text{C}\{^1\text{H}\}$ NMR (C_6D_6): δ 160.1, 155.8, 149.1, 147.1, 146.5, 138.6, 131.6, 129.2, 125.7, 125.3, 122.9 (q, $^1J_{\text{CF}} = 284.2$ Hz), 122.87, 122.84 (q, $^1J_{\text{CF}} = 284.9$ Hz), 122.6, 120.5, 79.2 (sep, $^2J_{\text{CF}} = 32.4$ Hz), 64.8, 28.0, 24.5, 17.9. ^{19}F NMR (C_6D_6): δ -76.11 (dd, $^2J_{\text{FF}} = 6.63$ and 40.2 Hz). Anal. Calcd for $\text{C}_{32}\text{H}_{34}\text{F}_{12}\text{N}_3\text{NbO}_2$: C, 47.24; H, 4.21; N, 5.17. Found: C, 47.04; H, 4.12; N, 5.10.

4.6. Synthesis of Nb(N-2-MeC₆H₄)[OCH(CF₃)₂]₂[2-(2,6-Me₂C₆H₃)NCH₂(C₅H₄N)] (3c). **4.6.1. Synthesis of Nb(N-2-MeC₆H₄)(NMe₂)₃ (1c).** Into a toluene solution (30 mL) containing Nb(NMe₂)₃ (500 mg, 1.59 mmol) was added toluene solution (10 mL) containing *o*-toluidine (171 mg, 1.59 mmol) at -78 °C. The mixture was stirred at -78 °C for 30 min, and the solution was warmed slowly to room temperature over 2 h. The mixture was then heated slowly to 70 °C over 2 h, and the solution was stirred at 80 °C for 1 h and at 90 °C for 1 h for completion. The reaction mixture was then placed in a rotary evaporator to remove the volatiles. The resultant oil was dissolved in *n*-hexane and the solution was passed through a celite pad, and the filtercake was washed with *n*-hexane. The combined filtrate and wash were placed in a rotary evaporator to remove the volatiles, and the resultant brown oil was confirmed as tris(dimethylamido) complex,

Nb(N-2-MeC₆H₄)(NMe₂)₃ (1c, 503 mg), confirmed by ^1H NMR spectrum (resonances assigned as formation of the desired complex). ^1H NMR (C_6D_6): δ 7.28 (d, 1H, $J = 7.75$, *Ar-H*), 7.06 (t, 1H, $J = 7.08$, *Ar-H*), 6.89–6.84 (m, 2H, *Ar-H*), 3.13 (s, 18H, $\text{N}(\text{CH}_3)_2$), 2.56 (s, 3H, *Ar-CH}_3*). The resultant sample was used for the next reaction without further purification.

4.6.2. Synthesis of Nb(N-2-MeC₆H₄)(NMe₂)₂[2-(2,6-Me₂C₆H₃)-NCH₂(C₅H₄N)] (2c). Into a *n*-hexane solution (30 mL) containing Nb(N-2-MeC₆H₄)(NMe₂)₃ (1c, 503 mg, 1.52 mmol) was added a *n*-hexane solution (8 mL) containing 2-(2,6-Me₂C₆H₃)N(H)-CH₂(C₅H₄N) (307 mg, 1.45 mmol) at -30 °C. The reaction mixture was warmed slowly to room temperature, and the mixture was then stirred overnight. The solution was passed through a Celite pad, and the filtercake was washed with *n*-hexane. The combined filtrate and wash were placed in a rotary evaporator to remove the volatiles, and the resultant dark brown oil was confirmed as bis(dimethylamido) complex, Nb(N-2-MeC₆H₄)(NMe₂)₂[2-(2,6-Me₂C₆H₃)-NCH₂(C₅H₄N)] (2c, 765 mg), confirmed by ^1H NMR spectra (resonances assigned as formation of the desired complex). ^1H NMR (C_6D_6): δ 8.27 (d, 1H, $J = 5.40$ Hz, *Ar-H*), 7.13 (t, 3H, $J = 7.53$ Hz, *Ar-H*), 7.06–6.96 (m, 3H, *Ar-H*), 6.81–6.77 (m, 2H, *Ar-H*), 6.49 (d, 1H, $J = 7.90$ Hz, *Ar-H*), 6.38 (t, 1H, $J = 6.40$ Hz, *Ar-H*), 4.50 (s, 2H, NCH_2), 3.11 (s, 12H, $\text{N}(\text{CH}_3)_2$), 2.45 (s, 6H, *Ar-CH}_3*), 2.43 (s, 3H, *Ar-CH}_3*). The resultant sample was used for the next reaction without further purification.

4.6.3. Synthesis of Nb(N-2-MeC₆H₄)[OCH(CF₃)₂]₂[2-(2,6-Me₂C₆H₃)-NCH₂(C₅H₄N)] (3c). Into a toluene solution (30 mL) containing Nb(N-2-MeC₆H₄)(NMe₂)₂[2-(2,6-Me₂C₆H₃)NCH₂(C₅H₄N)] (2c, 765 mg, 1.54 mmol) was added a toluene solution (8 mL) containing (CF₃)₂CHOH (409 mg, 2.43 mmol) slowly at -30 °C. The reaction mixture was warmed slowly to room temperature, and the mixture was then stirred for 3 h. The solution was passed through a celite pad, and the filtercake was washed with toluene. The combined filtrate and wash were placed in a rotary evaporator to remove the volatiles. The resultant oil was dissolved in a minimum amount of *n*-hexane. The chilled solution placed in the freezer (-30 °C) afforded white-brown microcrystals (357 mg, 0.504 mmol). Yield: 41.5%. ^1H NMR (C_6D_6): δ 8.51 (d, 1H, $J = 5.35$ Hz, *Ar-H*), 6.92 (d, 2H, $J = 7.50$ Hz, *Ar-H*), 6.83 (t, 1H, $J = 7.50$ Hz, *Ar-H*), 6.78 (t, 2H, $J = 5.85$ Hz, *Ar-H*), 6.72 (t, 1H, $J = 7.73$ Hz, *Ar-H*), 6.66 (t, 1H, $J = 7.43$ Hz, *Ar-H*), 6.44 (t, 1H, $J = 6.45$ Hz, *Ar-H*), 6.35 (d, 1H, $J = 8.05$ Hz, *Ar-H*), 6.24 (d, 1H, $J = 7.90$ Hz, *Ar-H*), 5.30 (sep, 2H, $J = 5.68$ Hz, $\text{CH}(\text{CF}_3)_2$), 4.27 (s, 2H, NCH_2), 2.29 (s, 6H, *Ar-CH}_3*), 2.26 (s, 3H, *Ar-CH}_3*). $^{13}\text{C}\{^1\text{H}\}$ NMR (C_6D_6): δ 159.7, 155.8, 152.9, 147.0, 138.4, 132.6, 131.8, 129.8, 128.8, 127.0, 125.9, 125.3, 124.7, 123.0 (q, $^1J_{\text{CF}} = 283.2$ Hz), 122.8 (q, $^1J_{\text{CF}} = 285.1$ Hz), 122.7, 120.4, 80.9 (sep, $^2J_{\text{CF}} = 32.2$ Hz), 64.3, 18.3, 18.0. ^{19}F NMR (C_6D_6): δ -75.87 (t, $^2J_{\text{FF}} = 6.96$ Hz), -76.07 . Anal. Calcd for $\text{C}_{27}\text{H}_{24}\text{F}_{12}\text{N}_3\text{NbO}_2$: C, 43.62; H, 3.25; N, 5.65. Found: C, 43.55; H, 3.13; N, 5.61.

4.7. Synthesis of Nb(N-2,6-Me₂C₆H₃)Me₂[2-(2,6-Me₂C₆H₃)-NCH₂(C₅H₄N)] (4a). Into a toluene solution (30 mL) containing Nb(N-2,6-Me₂C₆H₃)[OCH(CF₃)₂]₂[2-(2,6-Me₂C₆H₃)-NCH₂(C₅H₄N)] (3a, 533 mg, 0.704 mmol) was added a toluene solution (10 mL) containing MeMgBr (586 μL , 1.76 mmol, 3.0 M in diethyl ether) slowly at -30 °C. The reaction mixture was warmed slowly to room temperature, and the mixture was then stirred for 1 h. To the solution was added CH_2Cl_2 , and the mixture was placed in a rotary evaporator to remove the volatiles. The resultant residue was extracted with CH_2Cl_2 . The solution was passed through a celite pad, and the filtercake was washed with CH_2Cl_2 . The combined filtrate and wash were placed in a rotary evaporator to remove the volatiles. The resultant solid was dissolved in a minimum amount of CH_2Cl_2 and was layered with toluene. The chilled solution placed in the freezer (-30 °C) afforded yellow microcrystals (177 mg, 0.390 mmol). Yield: 55.5%. ^1H NMR (CDCl_3): δ 8.87 (d, 1H, $J = 5.25$ Hz, *Ar-H*), 7.97 (t, 1H, $J = 7.65$ Hz, *Ar-H*), 7.59 (t, 1H, $J = 6.40$ Hz, *Ar-H*), 7.52 (d, 1H, $J = 7.95$ Hz, *Ar-H*), 6.88 (d, 2H, $J = 7.50$ Hz, *Ar-H*), 6.80–6.74 (m, 3H, *Ar-H*), 6.61 (t, 1H, $J = 7.43$ Hz, *Ar-H*), 4.87 (s, 2H, NCH_2), 2.30 (s, 6H, *Ar-CH}_3*), 2.19

(s, 6H, Ar-CH₃), 0.56 (s, 6H, Nb-CH₃). ¹³C{¹H} NMR (CDCl₃): δ 162.2, 155.2, 153.3, 148.0, 137.9, 135.4, 131.9, 128.1, 126.7, 124.2, 123.1, 121.6, 121.3, 64.0, 40.5, 19.2, 18.4. Anal. Calcd for C₂₄H₃₀N₃Nb: C, 63.57; H, 6.67; N, 9.27. Found: C, 63.48; H, 6.58; N, 9.15.

4.8. Synthesis of Nb(N-2,6-ⁱPr₂C₆H₃)Me₂[2-(2,6-Me₂C₆H₃)-NCH₂(C₅H₄N)] (4b). Into a toluene solution (30 mL) containing Nb(N-2,6-ⁱPr₂C₆H₃)[OCH(CF₃)₂]₂[2-(2,6-Me₂C₆H₃)-NCH₂(C₅H₄N)] (3b, 400 mg, 0.492 mmol) was added a toluene solution (10 mL) containing MeMgBr (410 μL, 1.23 mmol, 3.0 M in diethyl ether) slowly at -30 °C. The reaction mixture was warmed slowly to room temperature, and the mixture was then stirred for 1 h. To the solution was added CH₂Cl₂, and the mixture was placed in a rotary evaporator to remove the volatiles. The resultant residue was extracted with CH₂Cl₂ and the solution was passed through a celite pad, and the filtercake was washed with CH₂Cl₂. The combined filtrate and wash were placed in a rotary evaporator to remove the volatiles. The resultant solid was dissolved in a minimum amount of CH₂Cl₂ and was layered with toluene. The chilled solution placed in the freezer (-30 °C) afforded yellow microcrystals (202 mg, 0.396 mmol). Yield: 80.6%. ¹H NMR (CDCl₃): δ 8.89 (d, 1H, J = 5.15 Hz, Ar-H), 7.97 (t, 1H, J = 7.25 Hz, Ar-H), 7.59 (t, 1H, J = 6.40 Hz, Ar-H), 7.51 (d, 1H, J = 7.95 Hz, Ar-H), 6.90–6.87 (m, 4H, Ar-H), 6.80 (t, 1H, J = 7.58 Hz, Ar-H), 6.71 (t, 1H, J = 7.50 Hz, Ar-H), 4.85 (s, 2H, NCH₂), 3.82 (sep, 2H, J = 6.80 Hz, CH(CH₃)₂), 2.18 (s, 6H, Ar-CH₃), 1.14 (d, 12H, J = 6.80 Hz, CH(CH₃)₂), 0.53 (s, 6H, Nb-CH₃). ¹³C{¹H} NMR (CDCl₃): δ 162.1, 154.8, 150.7, 148.1, 145.4, 137.8, 131.8, 128.2, 124.0, 123.1, 122.2, 121.6, 121.3, 64.3, 40.8, 27.8, 24.4, 18.1. Anal. Calcd for C₂₈H₃₈N₃Nb: C, 66.00; H, 7.52; N, 8.25. Found: C, 65.72; H, 7.29; N, 8.02.

4.9. Synthesis of Nb(N-2,6-MeC₆H₄)Me₂[2-(2,6-Me₂C₆H₃)-NCH₂(C₅H₄N)] (4c). Into a toluene solution (25 mL) containing Nb(N-2,6-MeC₆H₄)[OCH(CF₃)₂]₂[2-(2,6-Me₂C₆H₃)-NCH₂(C₅H₄N)] (3c, 302 mg, 0.406 mmol) was added a toluene solution (6 mL) containing MeMgBr (320 μL, 0.96 mmol, 3.0 M in diethyl ether) slowly at -30 °C. The reaction mixture was warmed slowly to room temperature, and the mixture was then stirred for 1 h. To the solution was added CH₂Cl₂, and the mixture was placed in a rotary evaporator to remove the volatiles. The resultant residue was extracted with CH₂Cl₂. The solution was passed through a celite pad, and the filtercake was washed with CH₂Cl₂. The combined filtrate and wash were placed in a rotary evaporator to remove the volatiles. The resultant solid was dissolved in a minimum amount of CH₂Cl₂ and was layered with toluene. The chilled solution placed in the freezer (-30 °C) afforded yellow microcrystals (90 mg, 0.205 mmol). Yield: 50.4%. ¹H NMR (CDCl₃): δ 8.88 (d, 1H, J = 5.20 Hz, Ar-H), 7.97 (t, 1H, J = 7.70 Hz, Ar-H), 7.59 (t, 1H, J = 6.40 Hz, Ar-H), 7.53 (d, 1H, J = 7.95 Hz, Ar-H), 6.98 (t, 3H, J = 8.73 Hz, Ar-H), 6.86 (t, 1H, J = 7.48 Hz, Ar-H), 6.76 (t, 1H, J = 7.45 Hz, Ar-H), 6.70 (t, 1H, J = 7.33 Hz, Ar-H), 6.06 (d, 1H, J = 7.70 Hz, Ar-H), 4.87 (s, 2H, NCH₂), 2.42 (s, 3H, Ar-CH₃), 2.20 (s, 6H, Ar-CH₃), 0.50 (s, 6H, Nb-CH₃). ¹³C{¹H} NMR (CDCl₃): δ 162.4, 155.7, 154.6, 147.9, 137.9, 133.9, 132.1, 129.0, 128.2, 125.6, 125.2, 124.2, 123.1, 121.8, 121.4, 64.0, 38.6, 18.8, 18.4. Anal. Calcd for C₂₃H₂₈N₃Nb: C, 62.87; H, 6.42; N, 9.56. Found: C, 61.95; H, 6.12; N, 9.36. Rather low C values would be due to incomplete combustion (formation of NbC) during the analysis run.

4.10. Synthesis of Nb(N-2,6-Me₂C₆H₃)(CH₂SiMe₂)₂[2-(2,6-Me₂C₆H₃)-NCH₂(C₅H₄N)] (5a). Into a toluene solution (10 mL) containing Nb(N-2,6-Me₂C₆H₃)[OCH(CF₃)₂]₂[2-(2,6-Me₂C₆H₃)-NCH₂(C₅H₄N)] (3a, 52 mg, 0.0686 mmol) was added a toluene solution (5 mL) containing Me₃SiCH₂MgCl (162 μL, 0.164 mmol, 1.0 M in diethyl ether) at -30 °C. The reaction mixture was warmed slowly to room temperature, and the mixture was then stirred for 1 h. To the solution was added CH₂Cl₂, and the mixture was placed in a rotary evaporator to remove the volatiles (addition of CH₂Cl₂ into the solution would improve the efficiency of the subsequent extraction). The resultant residue was extracted with CH₂Cl₂. The solution was passed through a celite pad, and the filtercake was washed with CH₂Cl₂. The combined filtrate and wash were placed in a rotary evaporator to remove the volatiles. The resultant solid was dissolved in a minimum amount of toluene and was layered with *n*-hexane. The chilled solution placed in the freezer (-30 °C) afforded yellow crystals of 5a (29 mg,

0.0485 mmol). Yield: 70.6%. ¹H NMR (C₆D₆): δ 8.75 (d, 1H, J = 5.10 Hz, Ar-H), 6.93 (d, 3H, J = 7.50 Hz, Ar-H), 6.89 (t, 2H, J = 7.28 Hz, Ar-H), 6.81 (t, 1H, J = 7.15 Hz, Ar-H), 6.72 (t, 1H, J = 7.55 Hz, Ar-H), 6.65 (t, 1H, J = 6.33 Hz, Ar-H), 6.54 (d, 1H, J = 8.05 Hz, Ar-H), 4.42 (s, 2H, NCH₂), 2.55 (s, 6H, Ar-CH₃), 2.21 (s, 6H, Ar-CH₃), 1.99 (d, 2H, J = 10.8 Hz, CH₂SiCH₃), 0.53 (d, 2H, J = 10.8 Hz, CH₂SiCH₃), 0.085 (s, 18H, CH₂SiCH₃). Anal. Calcd for C₃₀H₄₆N₃NbSi₂: C, 60.28; H, 7.76; N, 7.03. Found: C, 60.18; H, 7.67; N, 6.99.

4.11. Reaction of Nb(N-2,6-Me₂C₆H₃)Me₂[2-(2,6-Me₂C₆H₃)-NCH₂(C₅H₄N)] (4a) with Borate (6a). Into a Et₂O solution (10 mL) containing Nb(N-2,6-Me₂C₆H₃)Me₂[2-(2,6-Me₂C₆H₃)-NCH₂(C₅H₄N)] (4a, 20 mg, 0.0441 mmol) was added a Et₂O solution (4 mL) containing [Ph₃C][B(C₆F₅)₄] (40 mg, 0.0441 mmol) at -30 °C. The reaction mixture was warmed slowly to room temperature, and the mixture was then stirred for 1 h. After the reaction, the solution was placed in a rotary evaporator to remove the solvent. The residue was dissolved in Et₂O and dropped into *n*-hexane. Removal of the *n*-hexane layer and washing by *n*-hexane afforded the residue (33 mg). ¹H NMR (CDCl₃): δ 8.67 (d, 1H, J = 4.80 Hz, Ar-H), 8.17 (t, 1H, J = 7.80 Hz, Ar-H), 7.73 (d, 1H, J = 8.05 Hz, Ar-H), 7.67 (t, 1H, J = 6.50 Hz, Ar-H), 6.94 (d, 1H, J = 7.35 Hz, Ar-H), 6.90–6.82 (m, 4H, Ar-H), 6.76 (t, 1H, J = 7.48 Hz, Ar-H), 5.24 (d, 1H, J = 21.11 Hz, NCH₂), 5.16 (d, 1H, J = 21.10 Hz, NCH₂), 3.80 (br s, 8H, OCH₂CH₃), 2.31 (s, 6H, Ar-CH₃), 2.22 (s, 3H, Ar-CH₃), 2.13 (s, 3H, Ar-CH₃), 1.35 (s, 3H, Nb-CH₃), 1.32 (t, 12H, J = 6.85 Hz, OCH₂CH₃). ¹³C{¹H} NMR (CDCl₃): δ 161.3, 154.2, 151.6, 148.3 (br d, ¹J_{CF} = 240.5 Hz), 146.0, 141.5, 138.3 (br d, ¹J_{CF} = 245.1 Hz), 136.3 (br d, ¹J_{CF} = 239.7 Hz), 136.1, 130.6, 129.1, 128.9, 128.7, 127.6, 126.5, 125.7, 125.0, 123.3, 68.2, 65.7, 47.9, 19.1, 18.4, 18.3, 14.9 (signals ascribed to *ipso*-C₆F₅ carbon were not observed). ¹⁹F NMR (CDCl₃): δ -132.6, -162.9 (t, ³J_{FF} = 20.5 Hz), -166.8 (t, ³J_{FF} = 18.5 Hz). These NMR spectra strongly suggest the formation of the cationic methyl complex, [Nb(N-2,6-Me₂C₆H₃)Me₂{2-(2,6-Me₂C₆H₃)-NCH₂(C₅H₄N)}]⁺[B(C₆F₅)₄]⁻(Et₂O)₂ (6a), and the spectra are shown in the Supporting Information.

4.12. Reaction of Nb(N-2,6-ⁱPr₂C₆H₃)Me₂[2-(2,6-Me₂C₆H₃)-NCH₂(C₅H₄N)] (4b) with Borate (6b). Into a Et₂O solution (20 mL) containing Nb(N-2,6-ⁱPr₂C₆H₃)Me₂[2-(2,6-Me₂C₆H₃)-NCH₂(C₅H₄N)] (4b, 20 mg, 0.0392 mmol) was added a Et₂O solution (8 mL) containing [Ph₃C][B(C₆F₅)₄] (35 mg, 0.0392 mmol) at -30 °C. The reaction mixture was warmed slowly to room temperature, and the mixture was then stirred for 1 h. After the reaction, the solution was placed in a rotary evaporator to remove the solvent. The residue was dissolved in Et₂O and dropped into *n*-hexane. Removal of the *n*-hexane layer and washing by *n*-hexane afforded the residue (17 mg). ¹H NMR (CDCl₃): δ 8.50 (d, 1H, J = 5.35 Hz, Ar-H), 8.16 (t, 1H, J = 7.68 Hz, Ar-H), 7.72 (d, 1H, J = 7.95 Hz, Ar-H), 7.66 (t, 1H, J = 6.45 Hz, Ar-H), 6.93 (t, 5H, J = 8.30 Hz, Ar-H), 6.84 (t, 1H, J = 7.50 Hz, Ar-H), 5.22 (d, 1H, J = 21.16 Hz, NCH₂), 5.15 (d, 1H, J = 21.16 Hz, NCH₂), 3.63–3.57 (m, 2H, CH(CH₃)₂), 3.60 (br s, 8H, OCH₂CH₃), 2.24 (s, 3H, Ar-CH₃), 2.14 (s, 3H, Ar-CH₃), 2.13 (s, 3H, Ar-CH₃), 1.33 (s, 3H, Nb-CH₃), 1.30 (br s, 12H, OCH₂CH₃), 1.16 (dd, 12H, J = 6.98 and 9.65 Hz, CH(CH₃)₂). ¹³C{¹H} NMR (CDCl₃): δ 161.1, 153.8, 148.8, 148.3 (br d, ¹J_{CF} = 246.0 Hz), 146.7, 146.0, 141.5, 138.3 (br d, ¹J_{CF} = 241.5 Hz), 136.4 (br d, ¹J_{CF} = 240.0 Hz), 130.5, 129.3, 129.0, 128.9, 126.5, 126.4, 125.1, 123.3, 122.6, 66.1, 47.9, 28.4, 24.6, 24.1, 18.4, 18.0, 14.9 (signals ascribed to *ipso*-C₆F₅ carbon were not observed). ¹⁹F NMR (CDCl₃): δ -132.5, -162.8 (t, ³J_{FF} = 20.6 Hz), -166.8 (t, ³J_{FF} = 18.2 Hz). These NMR spectra strongly suggest the formation of the cationic methyl complex, [Nb(N-2,6-ⁱPr₂C₆H₃)Me₂{2-(2,6-Me₂C₆H₃)-NCH₂(C₅H₄N)}]⁺[B(C₆F₅)₄]⁻(Et₂O)₂ (6b), and the spectra are shown in the Supporting Information.

4.13. Oligomerization/Polymerization of ethylene. Ethylene oligomerizations were conducted in a 100 mL scale stainless steel autoclave. The typical reaction procedure is as follows. Toluene (29 mL) and the prescribed amount of MAO solid (prepared from ordinary MMAO-3AH by removing *n*-hexane, AlⁱBu₃ and AlMe₃) were added into the autoclave in the drybox. The reaction apparatus was then filled with ethylene (1 atm), and Nb(N-2,6-Me₂C₆H₃)Me₂[2-(2,6-Me₂C₆H₃)-NCH₂(C₅H₄N)] (4a) (3.0 μmol) in toluene (1.0 mL) was then added into the autoclave, the reaction apparatus was then

Table 5. Crystal Data and Collection Parameters of Nb(N-2,6-Me₂C₆H₃)[OCH(CF₃)₂]₂[2-(2,6-Me₂C₆H₃)NCH₂(C₅H₄N)] (3a), Nb(N-2,6-ⁱPr₂C₆H₃)[OCH(CF₃)₂]₂[2-(2,6-Me₂C₆H₃)NCH₂(C₅H₄N)] (3b), and Nb(N-2,6-ⁱPr₂C₆H₃)Me₂[2-(2,6-Me₂C₆H₃)NCH₂(C₅H₄N)] (4b), Nb(N-2-MeC₆H₄)Me₂[2-(2,6-Me₂C₆H₃)NCH₂(C₅H₄N)] (4c), and Nb(N-2,6-Me₂C₆H₃)(CH₂SiMe₃)₂[2-(2,6-Me₂C₆H₃)NCH₂(C₅H₄N)] (5a)^a

	3a	3b	4b	4c	5a
formula	C ₂₈ H ₂₆ F ₁₂ N ₃ NbO ₂	C ₃₂ H ₃₄ F ₁₂ N ₃ NbO ₂	C ₂₈ H ₃₈ N ₃ Nb	C ₂₃ H ₂₈ N ₃ Nb	C ₃₀ H ₄₆ N ₃ NbSi ₂
formula weight	757.42	813.53	509.53	439.39	597.79
crystal color, habit	colorless, plate	colorless, plate	colorless, plate	colorless, prism	orange, block
crystal size (mm)	0.130 × 0.110 × 0.070	0.100 × 0.070 × 0.040	0.100 × 0.080 × 0.040	0.120 × 0.080 × 0.030	0.150 × 0.150 × 0.130
crystal system	monoclinic	monoclinic	monoclinic	orthorhombic	monoclinic
space group	P2 ₁ /c (#14)	P2 ₁ /n (#14)	P2 ₁ /m (#11)	Pna2 ₁ (#33)	P2 ₁ /c (#14)
a (Å)	13.395(3)	9.7083(15)	8.7168(17)	22.844(3)	16.0468(5)
b (Å)	13.755(2)	18.057(3)	14.213(2)	8.4693(12)	11.8148(4)
c (Å)	16.964(3)	19.893(3)	10.837(2)	11.0164(16)	17.5487(6)
α (deg)	90	90	90	90	90
β (deg)	98.431(4)	98.516(4)	101.165(5)	90	103.113(3)
γ (deg)	90	90	90	90	90
V (Å ³)	3091.8(10)	3448.8(9)	1317.2(4)	2131.4(5)	3240.30(19)
Z value	4	4	2	4	4
D _{calcd} (g/cm ³)	1.627	1.567	1.285	1.369	1.225
F ₀₀₀	1520.00	1648.00	536.00	912.00	1264.00
temp (K)	93(2)	93(2)	93(2)	93(2)	93(2)
μ (Mo Kα) (cm ⁻¹)	4.928	4.477	4.760	5.76	4.669
no. of reflections measured (R _{int})	total: 24 285	total: 27 600	total: 10 690	total: 11 684	total: 23 086
	unique: 6463 (0.0323)	unique: 7420 (0.0448)	unique: 2832 (0.0225)	unique: 3920 (0.0227)	unique: 6516 (0.0524)
2θ _{max} (deg)	54.9	55.1	55.0	55.0	55.0
no. of observations [I > 2.00σ(I)]	6463	7420	2832	3920	6516
no. of variables	415	451	166	218	325
R1 [I > 2.00σ(I)]	0.0334	0.0325	0.0292	0.0316	0.0366
wR2 [I > 2.00σ(I)]	0.0966	0.0852	0.0776	0.0874	0.1035
goodness of fit	1.046	0.951	1.125	1.108	1.053

^aDetailed data are shown in the Supporting Information.¹⁶

immediately pressurized to 7 atm (total 8 atm), and the mixture was magnetically stirred for prescribed time. After the above procedure, ethylene remained was purged at -30 °C, and 100 μL of nonane was added as an internal standard. The solution was then analyzed by GC to determinate the activity and product distribution. In case of reaction in the presence of [Ph₃C][B(C₆F₅)₄], a toluene solution containing [Ph₃C][B(C₆F₅)₄] was added after injecting a toluene solution containing catalyst (4a). After the above oligomerization procedure, the remaining mixture in the autoclave was poured into MeOH containing HCl, and the resultant polymer (white precipitate) was collected on a filter paper by filtration and was adequately washed with MeOH. The resultant polymer was then dried in vacuo at 60 °C for 2 h.

4.14. Analysis of Catalyst Solution by Solution-Phase XAS. Nb K edge XANES measurements were carried out at the BL01B1 beamline at the SPring-8 facility of the Japan Synchrotron Radiation Research Institute (Nb K edge analysis, 18.98 keV, proposal no. 2018B1335). The measurements were conducted at room temperature. A Si (111) double-crystal monochromator was used for the incident beam. Nb K-edge XAFS spectra of Nb complex samples (prepared as toluene solution, 50 μmol/mL) were recorded in the fluorescence mode using an ionization chamber as the I₀ detector and 19 solid-state detectors as the I detector. The X-ray energy was calibrated using Nb foil; the XANES data were obtained by removing the background and normalization of them to the edge height.

4.15. Crystallographic Analysis. All measurements were made on a Rigaku XtaLAB P200 diffractometer using multilayer mirror monochromated Mo Kα radiation. The crystal collection parameters are listed below (Table 5). The data were collected and processed using CrystalClear (Rigaku)³¹ or CrysAlisPro (Rigaku Oxford Diffraction),³² and the structure was solved by direct methods³³ and expanded using Fourier techniques. The nonhydrogen atoms were refined anisotropi-

cally. Hydrogen atoms were refined using the riding model. All calculations were performed using the CrystalStructure³⁴ crystallographic software package, except for refinement, which was performed using SHELXL version 2014/7.^{35,36} Cif, xyz files are shown in the Supporting Information, and the crystallographic data were deposited to Cambridge Crystallographic Data Centre (CCDC 1887435–1887438, and CCDC 1889600).

■ ASSOCIATED CONTENT

Supporting Information

The Supporting Information is available free of charge on the ACS Publications website at DOI: 10.1021/acs.organo-
met.9b00017.

Additional results for reaction with ethylene using Nb(NAr)Me₂[2-(2,6-Me₂C₆H₃)NCH₂(C₅H₄N)] [Ar = 2,6-Me₂C₆H₃ (4a), 2,6-ⁱPr₂C₆H₃ (4b), 2-MeC₆H₄ (4c)]—cocatalyst systems and selected DSC thermograms and ¹H NMR spectra for PE byproduced; selected NMR spectra for prepared niobium(V) complexes and some reactions; and structural analysis for Nb(N-2-MeC₆H₄)Me₂[2-(2,6-Me₂C₆H₃)NCH₂(C₅H₄N)] (4c). (PDF)

CIF and xyz files for Nb(NAr)[OCH(CF₃)₂]₂[2-(2,6-Me₂C₆H₃)NCH₂(C₅H₄N)] [Ar = Me (3a, CCDC 1887435), ⁱPr (3b, CCDC 1887436)], Nb(N-2,6-ⁱPr₂C₆H₃)Me₂[2-(2,6-Me₂C₆H₃)NCH₂(C₅H₄N)] (4b, CCDC 1887437), Nb(N-2,6-Me₂C₆H₃)-(CH₂SiMe₃)₂[2-(2,6-Me₂C₆H₃)NCH₂(C₅H₄N)] (5a,

CCDC 1887438), and Nb(N-2-MeC₆H₄)Me₂[2-(2,6-Me₂C₆H₃)NCH₂(C₅H₄N)] (**4c**, CCDC 1889600). The supplemental files contain the computed Cartesian coordinates of all of the molecules reported in this study. The files may be opened as a text file to read the coordinates, or opened directly by a molecular modeling program such as Mercury (version 3.3 or later, <http://www.ccdc.cam.ac.uk/pages/Home.aspx>) for visualization and analysis (XYZ)

Accession Codes

CCDC 1887435–1887438 and 1889600 contain the supplementary crystallographic data for this paper. These data can be obtained free of charge via www.ccdc.cam.ac.uk/data_request/cif, or by emailing data_request@ccdc.cam.ac.uk, or by contacting The Cambridge Crystallographic Data Centre, 12 Union Road, Cambridge CB2 1EZ, UK; fax: +44 1223 336033.

AUTHOR INFORMATION

Corresponding Author

*E-mail: ktnomura@tmu.ac.jp. Phone: +81-42-677-2547. Fax: +81-42-677-2547.

ORCID

Kotohiro Nomura: 0000-0003-3661-6328

Notes

The authors declare no competing financial interest.

ACKNOWLEDGMENTS

This project was partly supported by Grant-in-Aid for Scientific Research from the Japan Society for the Promotion of Science (JSPS, no. 18H01982). Authors express their sincere thanks to Prof. S. Yamazoe (Tokyo Metropolitan University, TMU), Prof. T. Mitsudome (Osaka University), Dr. T. Ina (Japan Synchrotron Radiation Research Institute, JASRI), and I. Izawa, K. Kawamura, H. Hayashibara, H. Aoki (TMU) for XANES analysis at the BL01B1 beam line at the SPring-8 facility of JASRI (proposal no. 2018B1335). Authors also express their thanks to Dr. Ken Tsutsumi and Prof. A. Inagaki (TMU) for assistance in the crystallographic analysis and fruitful discussion and Prof. S. Komiya for discussion.

REFERENCES

(1) (a) Peuckert, M.; Keim, W. A new nickel complex for the oligomerization of ethylene. *Organometallics* **1983**, *2*, 594–597. (b) Peuckert, M.; Keim, W.; Storp, S.; Weber, R. S. ESCA and K-EDGE x-ray absorption spectroscopy applied to nickel one-component catalysts: A correlation between spectral data and the kinetics of linear olefin oligomerization. *J. Mol. Catal.* **1983**, *20*, 115–127. (c) Keim, W. Nickel: An element with wide application in industrial homogeneous catalysis. *Angew. Chem., Int. Ed. Engl.* **1990**, *29*, 235–244. (d) Keim, W. Oligomerization of Ethylene to α -Olefins: Discovery and Development of the Shell Higher Olefin Process (SHOP). *Angew. Chem., Int. Ed.* **2013**, *52*, 12492–12496.

(2) Selected reviews for metal catalyzed dimerization/oligomerization of ethylene, propylene, see: (a) Pillai, S. M.; Ravindranathan, M.; Sivaram, S. Dimerization of ethylene and propylene catalyzed by transition-metal complexes. *Chem. Rev.* **1986**, *86*, 353–399. (b) Skupinska, J. Oligomerization of α -olefins to higher oligomers. *Chem. Rev.* **1991**, *91*, 613–648. (c) Speiser, F.; Braunstein, P.; Saussine, L. Catalytic Ethylene Dimerization and Oligomerization: Recent Developments with Nickel Complexes Containing P,N-Chelating Ligands. *Acc. Chem. Res.* **2005**, *38*, 784–793. (d) McGuinness, D. S. Olefin oligomerization via metallacycles: Dimerization, trimerization, tetramerization, and beyond. *Chem. Rev.* **2011**, *111*, 2321–2341. (e) Agapie, T. Selective ethylene oligomerization: Recent advances in

chromium catalysis and mechanistic investigations. *Coord. Chem. Rev.* **2011**, *255*, 861–880. (f) van Leeuwen, P. W. N. M.; Clément, N. D.; Tschan, M. J.-L. New processes for the selective production of 1-octene. *Coord. Chem. Rev.* **2011**, *255*, 1499–1517. (g) Zhang, W.; Sun, W.-H.; Redshaw, C. Tailoring iron complexes for ethylene oligomerization and/or polymerization. *Dalton Trans.* **2013**, *42*, 8988–8997. (h) Wang, S.; Sun, W.-H.; Redshaw, C. Recent progress on nickel-based systems for ethylene oligo-/polymerization catalysis. *J. Organomet. Chem.* **2014**, *751*, 717–741. (i) Boudier, A.; Breuil, P.-A. R.; Magna, L.; Olivier-Bourbigou, H.; Braunstein, P. Ethylene oligomerization using iron complexes: beyond the discovery of bis(imino)pyridine ligands. *Chem. Commun.* **2014**, *50*, 1398–1407. (j) Small, B. L. Discovery and development of pyridine-bis(imine) and related catalysts for olefin polymerization and oligomerization. *Acc. Chem. Res.* **2015**, *48*, 2599–2611. (k) Wang, Z.; Solan, G. A.; Zhang, W.; Sun, W.-H. Carbocyclic-fused N,N,N-pincer ligands as ring-strain adjustable supports for iron and cobalt catalysts in ethylene oligo-/polymerization. *Coord. Chem. Rev.* **2018**, *363*, 92–108. (l) Bryliakov, K. P.; Antonov, A. A. Recent progress of transition metal based catalysts for the selective dimerization of ethylene. *J. Organomet. Chem.* **2018**, *867*, 55–61.

(3) For selected examples (oligomerization): (a) Reagan, W. K. (Phillips Petroleum Company) Process for Olefin Polymerization. EP 0417477 A2, 1991. (b) Killian, C. M.; Johnson, L. K.; Brookhart, M. Preparation of Linear α -Olefins Using Cationic Nickel(II) α -Diimine Catalysts. *Organometallics* **1997**, *16*, 2005–2007. (c) Svejda, S. A.; Brookhart, M. Ethylene Oligomerization and Propylene Dimerization Using Cationic (α -Diimine)nickel(II) Catalysts. *Organometallics* **1999**, *18*, 65–74. (d) Komon, Z. J. A.; Bu, X.; Bazan, G. C. Synthesis, characterization, and ethylene oligomerization action of [(C₆H₅)₂PC₆H₄C(O-B(C₆F₅)₃)O- κ^2 P,O]Ni(η^3 -CH₂C₆H₅). *J. Am. Chem. Soc.* **2000**, *122*, 12379–12380. (e) Small, B. L.; Brookhart, M. Iron-Based Catalysts with Exceptionally High Activities and Selectivities for Oligomerization of Ethylene to Linear α -Olefins. *J. Am. Chem. Soc.* **1998**, *120*, 7143–7144. (f) Britovsek, G. J. P.; Mastroianni, S.; Solan, G. A.; Baugh, S. P. D.; Redshaw, C.; Gibson, V. C.; White, A. J. P.; Williams, D. J.; Elsegood, M. R. J. Oligomerisation of ethylene by bis(imino)pyridyliron and -cobalt complexes. *Chem.—Eur. J.* **2000**, *6*, 2221–2231.

(4) Selected examples for Ti, Zr complex catalysts, see: (a) Wielstra, Y.; Gambarotta, S.; Chiang, M. Y. [1,2-Bis(dimethylphosphino)ethane](cyclopentadienyl)methylzirconium(II) [CpZrMe(DMPE)]₂: A catalyst precursor for the selective dimerization of ethylene to 1-butene. *Organometallics* **1988**, *7*, 1866–1867. (b) Deckers, P. J. W.; Hessen, B.; Teuben, J. H. Switching a catalyst system from ethene polymerization to ethene trimerization with a hemilabile ancillary ligand. *Angew. Chem., Int. Ed.* **2001**, *40*, 2516–2519. (c) Deckers, P. J. W.; Hessen, B.; Teuben, J. H. Catalytic Trimerization of Ethene with Highly Active Cyclopentadienyl-Arene Titanium Catalysts. *Organometallics* **2002**, *21*, 5122–5135. (d) You, Y.; Girolami, G. S. Mono(cyclopentadienyl)titanium(II) complexes with hydride, alkyl, and tetrahydroborate ligands: Synthesis, crystal structures, and ethylene dimerization and trimerization catalysis. *Organometallics* **2008**, *27*, 3172–3180. (e) Otten, E.; Batinas, A. A.; Meetsma, A.; Hessen, B. Versatile coordination of cyclopentadienyl-arene ligands and its role in titanium-catalyzed ethylene trimerization. *J. Am. Chem. Soc.* **2009**, *131*, 5298–5312. (f) Suzuki, Y.; Kinoshita, S.; Shibahara, A.; Ishii, S.; Kawamura, K.; Inoue, Y.; Fujita, T. Trimerization of Ethylene to 1-Hexene with Titanium Complexes Bearing Phenoxy-Imine Ligands with Pendant Donors Combined with MAO. *Organometallics* **2010**, *29*, 2394–2396. (g) Kinoshita, S.; Kawamura, K.; Fujita, T. Early-transition-metal catalysts with phenoxy-imine-type ligands for the oligomerization of ethylene. *Chem.—Asian J.* **2011**, *6*, 284–290.

(5) V complex catalysts, see: (a) Brussee, E. A. C.; Meetsma, A.; Hessen, B.; Teuben, J. H. The N,N'-bis(trimethylsilyl)-pentafluorobenzamidinate ligand: enhanced ethene oligomerisation with a neutral V(III) bis(benzamidinate) alkyl catalyst. *Chem. Commun.* **2000**, 497–498. (b) Schmidt, R.; Welch, M. B.; Knudsen, R. D.; Gottfried, S.; Alt, H. G. N,N,N-Tridentate iron(II) and vanadium(III) complexes Part II: Catalytic behavior for the oligomerization and

polymerization of ethene and characterization of the resulting products. *J. Mol. Catal. A: Chem.* **2004**, *222*, 17–25. Vanadium complexes containing chelate bis(imino)pyridine ligands yielded polymers/oligomers with Schultz–Flory distribution.

(6) (a) Zhang, S.; Nomura, K. Highly efficient dimerization of ethylene by (imido)vanadium complexes containing (2-anilidomethyl)pyridine ligands: Notable ligand effect toward activity and selectivity. *J. Am. Chem. Soc.* **2010**, *132*, 4960–4965. (b) Igarashi, A.; Zhang, S.; Nomura, K. Ethylene dimerization/polymerization catalyzed by (adamantylimido)vanadium(V) complexes containing (2-anilidomethyl)pyridine ligands: Factors affecting the ethylene reactivity. *Organometallics* **2012**, *31*, 3575–3581. (c) Nomura, K.; Igarashi, A.; Katao, S.; Zhang, W.; Sun, W.-H. Synthesis and structural analysis of (imido)vanadium(V) complexes containing chelate (anilido)methyl-imine ligands: Ligand effect in ethylene dimerization. *Inorg. Chem.* **2013**, *52*, 2607–2614. (d) Tang, X.-Y.; Igarashi, A.; Sun, W.-H.; Inagaki, A.; Liu, J.; Zhang, W.; Li, Y.-S.; Nomura, K. Synthesis of (imido)vanadium(V) complexes containing 8-(2,6-dimethylanilide)-5,6,7-trihydroquinoline ligands: Highly active catalyst precursors for ethylene dimerization. *Organometallics* **2014**, *33*, 1053–1060. (e) Nomura, K.; Mitsudome, T.; Igarashi, A.; Nagai, G.; Tsutsumi, K.; Ina, T.; Omiya, T.; Takaya, H.; Yamazoe, S. Synthesis of (adamantylimido)vanadium(V) dimethyl complex containing (2-anilidomethyl)pyridine ligand and selected reactions: Exploring the oxidation state of the catalytically active species in ethylene dimerization. *Organometallics* **2017**, *36*, 530–542.

(7) Selected examples, for ethylene oligomerization by niobium complex catalysts, (a) Schrock, R. R. Cyclooctatetraene Complexes of Niobium and Tantalum. U.S. Patent 3932477, du Pont de Nemours, E. I., and Co., USA, 1976. (b) Schrock, R. R.; Guggenberger, L. J.; English, A. D. Cyclooctatetraene complexes of niobium and tantalum and the structure of $\text{Nb}(\eta^4\text{-C}_8\text{H}_8)[\eta^5\text{-C}_8\text{H}_8(\text{C}_6\text{H}_5)][(\text{CH}_3)_2\text{AsC}_6\text{H}_4\text{As}(\text{CH}_3)_2]$. *J. Am. Chem. Soc.* **1976**, *98*, 903–913. (c) McLain, S. J.; Wood, C. D.; Schrock, R. R. Multiple metal-carbon bonds. 6. The reaction of niobium and tantalum neopentylidene complexes with simple olefins: a route to metallocyclopentanes. *J. Am. Chem. Soc.* **1977**, *99*, 3519–3520. (d) Chang, B.-H.; Lau, C.-P.; Grubbs, R. H.; Brubaker, C. H., Jr. Synthesis of polymer-attached niobium and tantalum complexes and their applications to the catalysis of olefin hydrogenation, isomerization and ethylene dimerization. *J. Organomet. Chem.* **1985**, *281*, 213–220.

(8) Ethylene oligomerization by tantalum catalysts,^{7a} see: (a) Fellmann, J. D.; Rupprecht, G. A.; Schrock, R. R. Rapid selective dimerization of ethylene to 1-butene by a tantalum catalyst and a new mechanism for ethylene oligomerization. *J. Am. Chem. Soc.* **1979**, *101*, 5099–5101. (b) Andes, C.; Harkins, S. B.; Murtuza, S.; Oyler, K.; Sen, A. New tantalum-based catalyst system for the selective trimerization of ethene to 1-hexene. *J. Am. Chem. Soc.* **2001**, *123*, 7423–7424. (c) Arteaga-Müller, R.; Tsurugi, H.; Saito, T.; Yanagawa, M.; Oda, S.; Mashima, K. New tantalum ligand-free catalyst system for highly selective trimerization of ethylene affording 1-hexene: New evidence of a metallacycle mechanism. *J. Am. Chem. Soc.* **2009**, *131*, 5370–5371. Ligand-free TaCl_5 -cocatalyst systems were used in the ref.^{8b,c}.

(9) For selected reviews, see: (a) Schrock, R. R. High Oxidation State Multiple Metal–Carbon Bonds. *Chem. Rev.* **2002**, *102*, 145–180. (b) Bolton, P. D.; Mountford, P. Transition metal imido compounds as Ziegler–Natta olefin polymerisation catalysts. *Adv. Synth. Catal.* **2005**, *347*, 355–366. (c) Schrock, R. R. Recent advances in high oxidation state Mo and W imido alkylidene chemistry. *Chem. Rev.* **2009**, *109*, 3211–3226. (d) Nomura, K.; Zhang, W. (Imido)vanadium(v)-alkyl-, -alkylidene complexes exhibiting unique reactivity towards olefins and alcohols. *Chem. Sci.* **2010**, *1*, 161–173. (e) Schrock, R. R. Synthesis of stereoregular polymers through ring-opening metathesis polymerization. *Acc. Chem. Res.* **2014**, *47*, 2457–2466. (f) Nomura, K.; Hou, X. Synthesis of vanadium-alkylidene complexes and their use as catalysts for ring opening metathesis polymerization. *Dalton Trans.* **2017**, *46*, 12–24.

(10) Synthesis and some reaction chemistry of half-sandwich niobium complexes containing arylimido ligands, see: (a) Williams, D. N.; Mitchell, J. P.; Poole, A. D.; Siemeling, U.; Clegg, W.; Hockless, D. C. R.; O’Neil, P. A.; Gibson, V. C. Half-sandwich imido complexes of niobium and tantalum. *J. Chem. Soc., Dalton Trans.* **1992**, 739–751. (b) Cockcroft, J. K.; Gibson, V. C.; Howard, J. A. K.; Poole, A. D.; Siemeling, U.; Wilson, C. η^2 -Benzynes and η^1 -benzylidene complexes of niobium with ancillary imido ligands. *J. Chem. Soc., Chem. Commun.* **1992**, 1668–1670. (c) Gibson, V. C. Ligands as “compass needles”: How orientations of alkene, alkyne, and alkylidene ligands reveal π -bonding features in tetrahedral transition metal complexes. *Angew. Chem., Int. Ed.* **1994**, *33*, 1565–1572. (d) Chan, M. C. W.; Cole, J. M.; Gibson, V. C.; Howard, J. A. K.; Lehmann, C.; Poole, A. D.; Siemeling, U. Half-sandwich imido complexes of niobium bearing alkyne, benzyne and benzylidene ligands: relatives of the zirconocene family. *J. Chem. Soc., Dalton Trans.* **1998**, 103–112. (e) Djakovitch, L.; Herrmann, W. A. Half-sandwich and *ansa*-niobiocenes: synthesis and reactivity. *J. Organomet. Chem.* **1998**, *562*, 71–78. (f) Humphries, M. J.; Green, M. L. H.; Leech, M. A.; Gibson, V. C.; Jolly, M.; Williams, D. N.; Elsegood, M. R. J.; Clegg, W. Niobium η -cyclopentadienyl compounds with imido and amido ligands derived from tert-butylamine. *J. Chem. Soc., Dalton Trans.* **2000**, 4044–4051. (g) Humphries, M. J.; Green, M. L. H.; Douthwaite, R. E.; Rees, L. H. Niobium- η -cyclopentadienyl compounds with imido and amido ligands derived from 2,6-dimethylaniline. *J. Chem. Soc., Dalton Trans.* **2000**, 4555–4562. (h) Antiñolo, A.; Dorado, I.; Fajardo, M.; Garcés, A.; López-Solera, I.; López-Mardomingo, C.; Kubicki, M. M.; Otero, A.; Prashar, S. Synthesis, structural characterisation and reactivity of new dinuclear monocyclopentadienyl imidoniobium and -tantalum complexes - X-ray crystal structures of $[\{\text{Nb}(\eta^5\text{-C}_5\text{H}_4\text{SiMe}_3)_2\text{Cl}_2(\mu\text{-1,4-NC}_6\text{H}_4\text{N})\}]$, $[\{\text{Ta}(\eta^5\text{-C}_5\text{Me}_5)_2\text{Cl}_2(\mu\text{-1,4-NC}_6\text{H}_4\text{N})\}]$ and $[\{\text{Ta}(\eta^5\text{-C}_5\text{Me}_5)(\text{CH}_2\text{SiMe}_3)_2(\mu\text{-1,4-NC}_6\text{H}_4\text{N})\}]$. *Eur. J. Inorg. Chem.* **2004**, 1299–1310. (i) Nikonov, G. I.; Mountford, P.; Dubberley, S. R. Tantalizing chemistry of the half-sandwich silylhydride complexes of niobium: Identification of likely intermediates on the way to agostic complexes. *Inorg. Chem.* **2003**, *42*, 258–260.

(11) Synthesis of the other (arylimido)niobium complexes, see: (a) Williams, D. S.; Thompson, D. W.; Korolev, A. V. The significant electronic effect of the imido alkyl substituent in d^0 group 5 imido compounds observed by luminescence in fluid solution at room temperature. *J. Am. Chem. Soc.* **1996**, *118*, 6526–6527. (b) Korolev, A. V.; Rheingold, A. L.; Williams, D. S. A general route to labile niobium and tantalum d^0 monoimides. Discussion of metal-nitrogen vibrational modes. *Inorg. Chem.* **1997**, *36*, 2647. (c) Herrmann, W. A.; Baratta, W.; Herdtweck, E. Multiple bonds between main-group elements and transition metals: Part 157 Neutral and cationic *ansa*-metallocenes of niobium(V) and tantalum(V): Synthesis, structures and stereochemical non-rigidity. *J. Organomet. Chem.* **1997**, *541*, 445–460. (d) Dorado, I.; Garcés, A.; López-Mardomingo, C.; Fajardo, M.; Rodríguez, A.; Antiñolo, A.; Otero, A. Synthesis and structural characterization of new organo-diimido and organo-imido niobium and titanium complexes. *J. Chem. Soc., Dalton Trans.* **2000**, 2375–2382. (e) Antiñolo, A.; Dorado, I.; Garcés, A.; López-Mardomingo, C.; Fajardo, M.; Kubicki, M.; Antiñolo, A.; Otero, A. Synthesis and structural characterisation of new organo-diimido tantalum and niobium complexes. *Dalton Trans.* **2003**, 910–917. (f) Elorriaga, D.; Carrillo-Hermosilla, F.; Antiñolo, A.; López-Solera, I.; Fernández-Galán, R.; Serrano, A.; Villaseñor, E. Synthesis, characterization and reactivity of new dinuclear guanidinate diimidoniobium complexes. *Eur. J. Inorg. Chem.* **2013**, 2940–2946. (g) Elorriaga, D.; Carrillo-Hermosilla, F.; Antiñolo, A.; López-Solera, I.; Fernández-Galán, R.; Villaseñor, E. Unexpected mild C–N bond cleavage mediated by guanidine coordination to a niobium iminocarbamoyl complex. *Chem. Commun.* **2013**, *49*, 8701–8703. (h) Elorriaga, D.; Carrillo-Hermosilla, F.; Antiñolo, A.; López-Solera, I.; Fernández-Galán, R.; Villaseñor, E. Mixed amido-/imido-/guanidinato niobium complexes: synthesis and the effect of ligands on insertion reactions. *Dalton Trans.* **2014**, *43*, 17434–17444. (i) Wised, K.; Nomura, K. Synthesis of (imido)niobium(V)-alkylidene complexes that exhibit high catalytic activities for metathesis polymer-

ization of cyclic olefins and internal alkynes. *Organometallics* **2016**, *35*, 2773–2777. (j) Srisupap, N.; Wised, K.; Tsutsumi, K.; Nomura, K. Synthesis of (Arylimido)niobium(V) Complexes Containing Ketimide, Phenoxide Ligands, and Some Reactions with Phenols and Alcohols. *ACS Omega* **2018**, *3*, 6166–6181.

(12) These data were partly presented at The 19th IUPAC International Symposia on Organometallic Chemistry Directed Towards Organic Synthesis (OMCOS19), Jeju, Korea, June, 2017. *International Symposium on Catalysis and Fine Chemicals 2018 (C&FC2018)*, Bangkok, Thailand, December, 2018.

(13) Unpublished results in the reactions of Nb(NAr)Cl₃(dme) or Nb(NAr)(OTf)₃(dme) (dme = 1,2-dimethoxyethane, Tf = CF₃SO₃) with 2-(2,6-Me₂C₆H₃)N(H)CH₂(C₅H₄N) by Srisupap, N. Related results, reactions of Nb(NAr)Cl₃(dme) with lithium phenoxide, are also shown in ref 11j.

(14) Selected NMR spectra for the prepared complexes (**2a,b**, **3a,b**, **4a,b**, **5a** and **6a,b**), and some reactions are shown in the [Supporting Information](#).

(15) For examples (Zr and Hf complexes), see: (a) Liang, L.-C.; Schrock, R. R.; Davis, W. M. Synthesis of titanium, zirconium, and hafnium complexes that contain the [(mesitylN-*o*-C₆H₄)₂O]²⁻ ligand. *Organometallics* **2000**, *19*, 2526–2531. (b) Evans, L. T. J.; Coles, M. P.; Geoffrey, F.; Cloke, N.; Hitchcock, P. B. Deactivation pathways of ethylene polymerization catalysts derived from titanium and zirconium 1,3-bis(furyl)-1,1,3,3-tetramethyldisilazide complexes. *Dalton Trans.* **2007**, 2707–2717.

(16) Cif, xyz files for structural analysis of Nb(NAr)[OCH(CF₃)₂]2[2-(2,6-Me₂C₆H₃)NCH₂(C₅H₄N)] [Ar = Me (**3a**), ⁱPr (**3b**)], Nb(N-2,6-ⁱPr₂C₆H₃)Me₂[2-(2,6-Me₂C₆H₃)NCH₂(C₅H₄N)] (**4b**), Nb(N-2,6-Me₂C₆H₃)(CH₂SiMe₃)₂[2-(2,6-Me₂C₆H₃)NCH₂(C₅H₄N)] (**5a**) are shown in the [Supporting Information](#). Structure of Nb(N-2-MeC₆H₄)Me₂[2-(2,6-Me₂C₆H₃)NCH₂(C₅H₄N)] (**4c**) was also confirmed by X-ray crystallographic analysis (with additional note), and the ORTEP drawing and the basic analysis data (with notes) are shown in the [Supporting Information](#).

(17) For examples, (a) Crans, D. C.; Tarlton, M. L.; McLaughlan, C. C. Trigonal bipyramidal or square pyramidal coordination geometry? Investigating the most potent geometry for vanadium phosphatase inhibitors. *Eur. J. Inorg. Chem.* **2014**, 4450–4468. (b) Addison, A. W.; Rao, T. N.; Reedijk, J.; van Rijn, J.; Verschoor, G. C. Synthesis, structure, and spectroscopic properties of copper(II) compounds containing nitrogen-sulphur donor ligands; the crystal and molecular structure of aqua[1,7-bis(N-methylbenzimidazol-2'-yl)-2,6-dithiaheptane]copper(II) perchlorate. *Dalton Trans.* **1984**, 1349–1356.

(18) Zhang, S.; Katao, S.; Sun, W.-H.; Nomura, K. Synthesis of (Arylimido)vanadium(V) Complexes Containing (2-Anilidomethyl)pyridine Ligands and Their Use as the Catalyst Precursors for Olefin Polymerization. *Organometallics* **2009**, *28*, 5925–5933.

(19) Additional results for reaction with ethylene using Nb(NAr)Me₂[2-(2,6-Me₂C₆H₃)NCH₂(C₅H₄N)] [Ar = 2,6-Me₂C₆H₃] (**4a**), 2,6-ⁱPr₂C₆H₃] (**4b**), 2-MeC₆H₄] (**4c**)]–cocatalyst systems, DSC thermograms and ¹H NMR spectrum in the resultant polyethylene by-produced are shown in the [Supporting Information](#).

(20) For examples (significant decrease in the catalytic activities in toluene), see: (a) Scollard, J. D.; McConville, D. H.; Payne, N. C.; Vittal, J. J. Polymerization of α -Olefins by Chelating Diamide Complexes of Titanium. *Macromolecules* **1996**, *29*, 5241–5243. (b) Wang, W.; Fujiki, M.; Nomura, K. Ethylene polymerization catalyzed by titanium(IV) complexes with triaryloxoamine ligand of type, TiX[(OArCH₂)₃N. *Macromol. Rapid Commun.* **2004**, *25*, 504–507. (c) Omiya, T.; Natta, S.; Wised, K.; Tsutsumi, K.; Nomura, K. Synthesis and structural analysis of niobium(V) complexes containing amine triphenolate ligands of the type, [NbCl(X)(O-2,4-R₂C₆H₂-6-CH₂)₃N] (R = Me, ^tBu; X = Cl, CF₃SO₃), and their use in catalysis for ethylene polymerization. *Polyhedron* **2017**, *125*, 9–17.

(21) Motolko, K. S. A.; Price, J. S.; Emslie, D. J. H.; Jenkins, H. A.; Britten, J. F. Zirconium complexes of a rigid, dianionic pincer ligand:

Alkyl cations, arene coordination, and ethylene polymerization. *Organometallics* **2017**, *36*, 3084–3093.

(22) Dixon, R. E.; Streitwieser, A. The kinetic acidity of 1,1,1-triphenylethane. *J. Org. Chem.* **1992**, *57*, 6125–6128.

(23) For example, see: (a) Li, J.; Yang, X.; Stern, C. L.; Marks, T. J. Cationic metallocene polymerization catalysts based on tetrakis-(pentafluorophenyl)borate and its derivatives. probing the limits of anion “noncoordination” via a synthetic, solution dynamic, structural, and catalytic olefin polymerization study. *Organometallics* **1997**, *16*, 842–857. (b) Keaton, R. J.; Jayaratne, K. C.; Fettinger, J. C.; Sita, L. R. Structural Characterization of Zirconium Cations Derived from a Living Ziegler–Natta Polymerization System: New Insights Regarding Propagation and Termination Pathways for Homogeneous Catalysts. *J. Am. Chem. Soc.* **2000**, *122*, 12909–12910. (c) Nomura, K.; Fudo, A. A study concerning the effect of organoboron compounds in 1-hexene polymerization catalyzed by Cp*TiMe₂(O-2,6-ⁱPr₂C₆H₃). Structural analysis for Cp*TiMe₂(O-2,6-ⁱPr₂C₆H₃) and Cp*TiMe(CF₃SO₃)(O-2,6-ⁱPr₂C₆H₃). *Inorg. Chim. Acta* **2003**, *345*, 37–43. (d) Lee, H.; Jordan, R. F. Unusual reactivity of tris(pyrazolyl)borate zirconium benzyl complexes. *J. Am. Chem. Soc.* **2005**, *127*, 9384–9385. (e) Lee, H.; Nienkemper, K.; Jordan, R. F. Synthesis and reactivity of a sterically crowded tris(pyrazolyl)borate hafnium benzyl complex. *Organometallics* **2008**, *27*, 5075–5081. (f) Nienkemper, K.; Lee, H.; Jordan, R. F.; Ariafard, A.; Dang, L.; Lin, Z. Synthesis of double-end-capped polyethylene by a cationic tris(pyrazolyl)borate zirconium benzyl complex. *Organometallics* **2008**, *27*, 5867–5875. (g) Itagaki, K.; Kakinuki, K.; Katao, S.; Khamnaen, T.; Fujiki, M.; Nomura, K.; Hasumi, S. Tris(pyrazolyl)borate Ti(IV) complexes containing phenoxy ligands: Effective catalyst precursors for ethylene polymerization that proceeds via cationic Ti(IV) species. *Organometallics* **2009**, *28*, 1942–1949. (h) Hasumi, S.; Itagaki, K.; Zhang, S.; Nomura, K. Ethylene polymerization by phenoxy substituted tris(pyrazolyl)borate Ti(IV) methyl complexes. *Macromolecules* **2011**, *44*, 773–777.

(24) Example of role of Al(*n*-C₈H₁₇)₃ as a scavenger, see: (a) Nomura, K.; Fudo, A. Efficient living polymerization of 1-hexene by Cp*TiMe₂(O-2,6-ⁱPr₂C₆H₃)-borate catalyst systems at low temperature. *J. Mol. Catal. A: Chem.* **2004**, *209*, 9–17. (b) Nomura, K.; Suzuki, N.; Kim, D.-H.; Kim, H. J. Effect of Cocatalyst in Ethylene/Styrene Copolymerization by Aryloxo-Modified Half-Titanocene-Cocatalyst Systems for Exclusive Synthesis of Copolymers at High Styrene Concentrations. *Macromol. React. Eng.* **2012**, *6*, 351–356.

(25) It seems that percentage of PE by-produced was rather high, probably due to partial decomposition of the catalytically-active species in the solution (without stabilization by MAO), as observed in ref 23h.

(26) As described in ref.^{23e,g,h} Al(*n*-C₈H₁₇)₃ or MAD [MeAl(O-2,6-ⁱBu-4-MeC₆H₂)₃] are known to be employed as scavenger (removal of impurities in solution), and Al(*n*-C₈H₁₇)₃ was employed for cleavage of the coordinated solvent (THF).^{23g,h} The Al alkyl would also play a role to stabilize the catalytically active species for the subsequent decomposition by reacting with borate. Reported examples^{23c,g,h} for polymerization of α -olefin or styrene with dialkyl complexes in the presence of borate and Al(*n*-C₈H₁₇)₃, see: (a) Hagihara, H.; Shiono, T.; Ikeda, T. Living polymerization of propene and 1-hexene with the [*t*-BuNSiMe₂Flu]TiMe₂/B(C₆F₅)₃ catalyst. *Macromolecules* **1998**, *31*, 3184–3188. They proposed that Al(*n*-C₈H₁₇)₃ interacts with the counteranion of the cationic active Ti species to improve coordinative unsaturation of the Ti species. (b) Fukui, Y.; Murata, M.; Soga, K. Living polymerization of propylene and 1-hexene using bis-Cp type metallocene catalysts. *Macromol. Rapid Commun.* **1999**, *20*, 637. (c) Beckerle, K.; Manivannan, R.; Spaniol, T. P.; Okuda, J. Living isospecific styrene polymerization by chiral benzyl titanium complexes that contain a tetradentate [OSSO]-type bis(phenolato) ligand. *Organometallics* **2006**, *25*, 3019–3026.

(27) For example, *XAFS Techniques for Catalysts, Nanomaterials, and Surfaces*; Iwasawa, Y., Asakura, K., Tada, M., Eds.; Springer: Switzerland, 2017.

(28) Related examples for analysis of catalytically active species by solution-phase V K-edge XAS analysis.^{6c} (a) Nagai, G.; Mitsudome, T.; Tsutsumi, K.; Sueki, S.; Ina, T.; Tamm, M.; Nomura, K. Effect of Al

cocatalyst in ethylene and ethylene/norbornene (Co)polymerization by (imido)vanadium dichloride complexes containing anionic *N*-heterocyclic carbenes having weakly coordinating borate moiety. *J. Jpn. Pet. Inst.* **2017**, *60*, 256–262. (b) Nomura, K.; Oshima, M.; Mitsudome, T.; Harakawa, H.; Hao, P.; Tsutsumi, K.; Nagai, G.; Ina, T.; Takaya, H.; Sun, W.-H.; Yamazoe, S. Synthesis and Structural Analysis of (Imido)vanadium Dichloride Complexes Containing 2-(2'-Benzimidazolyl)pyridine Ligands: Effect of Al Cocatalyst for Efficient Ethylene (Co)polymerization. *ACS Omega* **2017**, *2*, 8660–8673. (c) Nomura, K.; Tsutsumi, K.; Nagai, G.; Omiya, T.; Ina, T.; Yamazoe, S.; Mitsudome, T. Solution XAS analysis of various (imido)vanadium(V) dichloride complexes containing monodentate anionic ancillary donor ligands: Effect of aluminium cocatalyst in ethylene/norbornene (co)polymerization. *J. Jpn. Pet. Inst.* **2018**, *61*, 282–287.

(29) For example (account), Yamamoto, T. Assignment of pre-edge peaks in K-edge x-ray absorption spectra of 3d transition metal compounds: electric dipole or quadrupole? *X-Ray Spectrom.* **2008**, *37*, 572–584. The transition of a 1s electron to 3d orbital gives weak pre-edge peaks due to the electric quadrupole transition for any symmetries. An intense pre-edge peak is assigned to an electric dipole transition to p-character in the d–p hybridized orbital, and the mixing of a metal 4p orbital with the 3d orbital strongly depends on the coordination symmetry.

(30) (a) Srivastava, U. C.; Nigam, H. L. X-ray absorption edge spectrometry (xaes) as applied to coordination chemistry. *Coord. Chem. Rev.* **1973**, *9*, 275–310. References cited therein. (b) Asakura, H.; Shishido, T.; Yamazoe, S.; Teramura, K.; Tanaka, T. Structural analysis of group V, VI, and VII metal compounds by XAFS. *J. Phys. Chem. C* **2011**, *115*, 23653–23663. (c) Nomura, K.; Mitsudome, T.; Tsutsumi, K.; Yamazoe, S. Solution XAS analysis for exploring the active species in homogeneous vanadium complex catalysis. *J. Phys. Soc. Jpn.* **2018**, *87*, 061014.

(31) *CrystalClear: Data Collection and Processing Software*; Rigaku Corporation (1998–2015): Tokyo 196-8666, Japan, 2015.

(32) *CrysAlisPro: Data Collection and Processing Software*; Rigaku Corporation (2015): Tokyo 196-8666, Japan, 2015.

(33) Sheldrick, G. SHELXT: Integrating space group determination and structure solution. *Acta Crystallogr., Sect. A: Found. Adv.* **2014**, *70*, C1437.

(34) *CrystalStructure 4.2: Crystal Structure Analysis Package*; Rigaku Corporation (2000–2015): Tokyo 196-8666, Japan; 2000–2015.

(35) SHELXL Version 2014/7: Sheldrick, G. M. A short history of SHELX. *Acta Crystallogr., Sect. A: Found. Crystallogr.* **2008**, *64*, 112–122.

(36) Sheldrick, G. M. Crystal structure refinement with SHELXL. *Acta Crystallogr., Sect. C: Struct. Chem.* **2015**, *71*, 3–8.